UNIVERSITY OF CALIFORNIA, MERCED

INVESTIGATION OF A PROLYLS TRANS-CIS ISOMERIZATION OF METAMORPHIC CIRCADIAN CLOCK PROTEIN KAIB

A thesis submitted in partial satisfaction of the requirements for the degree of Master of Science

In

Chemistry and Chemical Biology

By

Alicia Vazquez

Committee in charge:

Dr. Victor Muñoz, Chair

Dr. Andy LiWang, Advisor

Dr. Patricia LiWang

Dr. Jing Xu

2017

Thesis of Alicia Vazquez is approved, and it is acceptable in quality and form for publication of microfilm and electronically:

Dr. Victor Muñoz (Chair)	Chemistry and Chemical Biology
Dr. Andy LiWang	Chemistry and Chemical Biology
Dr. Patricia LiWang	Chemistry and Chemical Biology
Dr. Jing Xu	Physics

ABSTRACT

INVESTIGATION OF A PROLYLS TRANS-CIS ISOMERIZATION OF METAMORPHIC CIRCADIAN CLOCK PROTEIN KAIB

Circadian clocks are universal among living organisms. In humans, circadian clock serve two main function; (1) promote daytime responses such as physical and mental activity and the biochemical and cardiovascular changes associated with them and (2) to enable preparation between the active and resting phases. To better understand how circadian clocks exert these functions it is necessary to study the molecular mechanism governing them. The circadian clock of cyanobacteria is a good model for studying such mechanisms due to its simplicity and ability to be reconstituted *in vitro*. Of the three core oscillating proteins, KaiA, KaiB, and KaiC, KaiB is a unique metamorphic protein that undergoes a fold-switching mechanism allowing KaiB to sample two native folds. Comparison of these folds revealed three prolyl trans-to-cis isomerase residues. To elucidate the mechanism behind KaiB fold switching, mutagenesis of the three proline residues to alanine was applied. It is hypothesized that removing the prolyl trans-cis isomerization will cause KaiB to become more stable by restricting fold switching. Differential scanning calorimetry of the proline to alanine mutants showed destabilization of proline70 to alanine suggesting Pro70 may act as a molecular hinge. NMR relaxation experiments were optimized for future studies on the destabilizing effect of Pro70 to alanine and its role as a potential molecular hinge.

Alicia Vazquez

August 2017

ACKNOWLEDGEMENTS

I would like thank my advisor Dr. Andy LiWang for his guidance and support over the last 18 months. He has been patient and provided endless information and resources with a constant positive attitude. I would also like to thank Dr. YongGang Chang, Dr. Archana Chavan, and PhD candidate Joel Heisler who have all been instrumental in proper lab etiquette, trouble shooting, and support. I am grateful to have had an opportunity to work alongside everyone in the LiWang lab. They taught me how important it is to be detailed oriented, to ask questions, to be curious, but most of all, to enjoy the scientific process.

I would also like extend my deepest gratitude to my parents who have worked tirelessly to provide me with all the resources needed for me to pursue a higher education. Lastly, I would like to dedicate this to the three smartest girls I know, Luna, Violet, and Olive. I can't wait to see what the three of you accomplish.

TABLE OF CONTENTS

LIST OF FIGURES, GRAPHS, & TABLES

CHAPTER 1: INTRODUCTION

Ch 1.1 THE CIRCADIAN CLOCK OF CYANOBACTERIA

The necessity to track time of day has always captured our attention. From the sun governing daily life and survival for Paleolithic humans to modern atomic clocks, we still rely on a 24-hour rhythm to cope with daily changes in our environment. Our biological (circadian) clocks still follow a 24-hour rhythm. For instance, hormones like cortisol and testosterone are highest in the morning while melatonin and prolactin reach their maximum during sleep hours [(14)]. Much like humans, other living organisms including bacteria, fungi, plants, insects, and mammals have also evolved circadian clocks in anticipation of day-to-night changes for enhancing fitness [(14)]. For example, plants with a circadian rhythm matched to the environment fix more carbon, contain more chlorophyll, and grow faster, providing a competitive advantage to plants with a circadian rhythm differing from their environment [(13)]. All circadian clock share three main characteristics; (1) temperature compensation of the period, (2) phase resetting by light or dark, and (3) an endogenous, near 24-hour cycle [(14)]. To understand how circadian clocks function, it is essential to study the molecular mechanism governing these rhythms. The circadian clock of the cyanobacterium *Synechococcus elongatus*, is ideal for such mechanistic studies because, in contrast to all other known circadian clocks, which utilize transcription-translation based feedback mechanisms, it is a post-translational clock, consisting of only three proteins, and can be reconstituted *in vitro* by combining its three components [(50)].

The three core oscillator proteins KaiA, KaiB, and KaiC (fig.1.1) (Kai meaning cycle in Japanese) are encoded by their respective genes *kaiA, kaiB, and kaiC* [45]. These three genes are responsible for timing of cell division [48, 74], gene expression [45, 37], and compaction of the chromosome [58]. As the sun rises, KaiA binds to unphosphorylated KaiC [88]. The binding of KaiA to KaiC stimulates KaiC autophosphorylation [78] first at residue Threonine-432 (T432) and then at Serine- 431 (S431) [89]. In the evening, S431 phosphorylation of KaiC allows for binding of KaiB [87] Once bound to KaiC, KaiB sequesters KaiA to allow KaiC to begin autodephosphorylation [87]. A new cycle begins the following morning (fig. 1.2).

The cyanobacterial circadian clock is governed by the enzymatic kinase and phosphatase activity of KaiC. KaiC kinase and phosphatase activities are at the core of generating its 24-hour phosphorylation rhythm under regulation of KaiA and KaiB [73]. KaiC is a double-donut shaped hexamer with two homologous domains, CI (N-terminal) and CII (C-terminal) (fig 1.1C) [56], and belongs to the AAA+ (ATPase Associated with diverse cellular Activities) family [83]. At the CI and CII subunit interfaces, the ATPase activity of KaiC hydrolyzes ATP. However, autokinase activity occurs only in the CII domain [53]. With both phosphorylation and dephosphorylation mediated by a phosphotransfer reaction on the CII subunit, KaiC begins its cycle with un-phosphorylated residues S431 and T432 (ST) approximately around dawn [73: 53]. The cycle proceeds as follows, ST→ SpT → pSpT → pST → ST [89, 50]. For the two states (ST and SpT) of KaiC where S431 is not phosphorylated, the CII ring is undergoing breathing motions and the CI and CII rings are un-stacked [87]. Following the phosphorylation of S431 (pSpT and pST), stacking occurs and the CII ring tightens, exposing the KaiB binding site on CI [87]. The

breathing motions of the CII (ST, SpT) ring allow for CI ATPase activity and binding of KaiA. Upon CII ring tightening (pSpT, pST), ATPase activity is suppressed, and binding of KaiB is promoted [28, 87].

The CII A-loop is the regulator of KaiC enzymatic activity. It exists in an equilibrium between exposed and buried positions, exposed A-loops promote KaiC autokinase activity while buried A-loops promote KaiC autophosphatse activity [88]. During the subjective day, the A-loop of KaiC (ST, SpT) can sample the exposed and buried positions. The C-terminal of KaiA stabilizes the A-loop in the exposed position, stimulating KaiC autophosphorylation [69, 55]. When the A-loops are in their buried position, the KaiA-KaiC interactions are weakened [8, 78]. Concurrently, N-terminal SasA will bind to the B-loops on the CI domain of KaiC [78], leading to the phosphorylation of the transcription factor and response regulator RpaA [23, 18]. The C-terminal of SasA contains a phosphorylation site that is enhanced when bound to KaiC [58, 81]. Once phosphorylated, SasA transfers its newly obtained phosphate group to RpaA [81, 51]. The two-component SasA-RpaA regulatory system is the main output for coordinating circadian gene expression for the correct period length, phase relationship, and robust oscillation for KaiC phosphorylation [23, 51]. As the cycle progresses and the onset of darkness begins (pSpT) KaiA autoinhibits itself upon KaiABC ternary complex formation, blocking stimulation of KaiC phosphorylation [79].

In the evening, when KaiC is hyperphosphorylated (pSpT), its CI and CII rings stack [88], promoting KaiB-CI binding [87], which sequesters KaiA in the KaiC-KaiB-KaiA ternary complex. Furthermore, KaiC phosphorylation at Ser431 also directly weakens

KAiC-KaiA interactions, which facilitates KaiA inhibition [78]. In addition to its pivotal role in the day/night switch of the oscillator, the KaiC-KaiB complex binds and activates the nighttime output signaling protein CikA [18]. Stacking of the CI and CII rings exposes the B-loops on the CI subunit of KaiC allowing it to capture KaiB [87, 78]. KaiB and the N-terminal of SasA have a similar sequence and bind to the same location on KaiC [22]. Though SasA can bind each phosphoform of KaiC, KaiB can compete for binding to CI when the KaiC rings are stacked and thus displacing SasA [78]. However, before KaiB can bind CI it must first undergo a conformational, or fold switch, mechanism [9]. KaiB has two tertiary structures, one active (fold switch) and one inactive (ground state). In its fold switch (fs) form KaiB is a monomer with a thioredoxin-like fold, like that of N-terminal SasA [9] and a homotetramer in its ground state (gs) form [19]. fsKaiB binds to CI in a 1:1 ratio forming a ring-like structure on the bottom face of the CI domain [79]. After fs-KaiB is captured by CI in its post-ATP hydrolysis state, fs-KaiB sequesters KaiA in its closed conformation halting autokinase stimulation [79, 69]. KaiA and CikA compete for binding to fs-KaiB [10]. When bound to fs-KaiB, CikA promotes the accumulation of unphosphorylated RpaA [67, 18]. At dawn KaiC fully dephosphorylates (ST), causing ternary complexes KaiA-KaiB-KaiC and CikA-KaiB-KaiC to dissociate, and begin a new cycle [79].

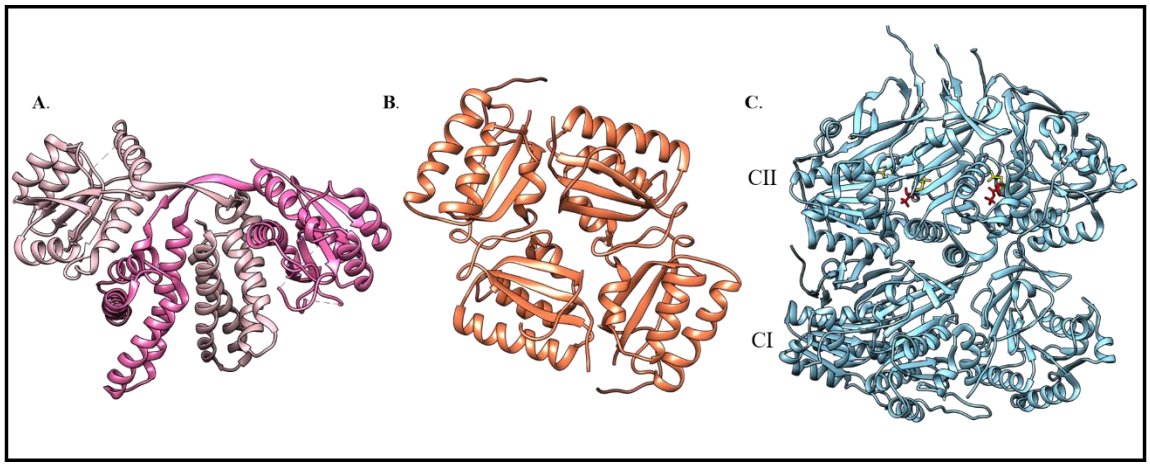

Figure 1.1: (A) KaiA (65KDa). The domain swapped homodimer subunits are shown in pink and hot pink. (B) Tetrameric gsKaiB (48KDa) is shown in coral. (C) KaiC (345KDa) is shown in light blue with the S431 and T432 phospho-residues in yellow and red, respectively, shown in the CII domain.

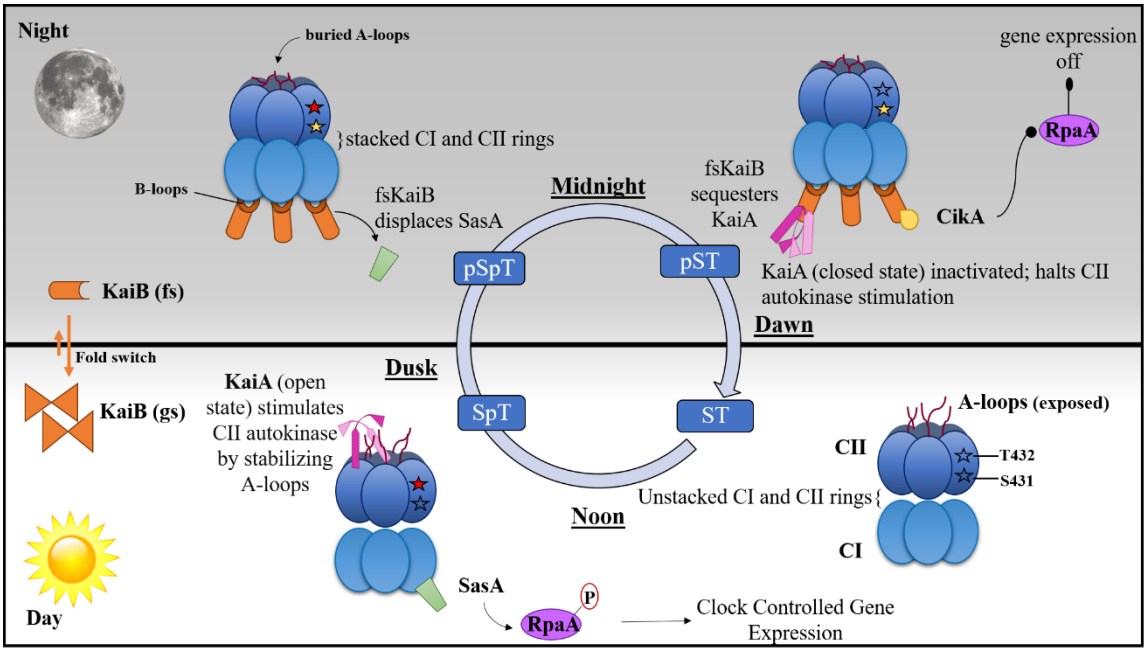

Figure 1.2: A cartoon representation of the cyanobacterial oscillator. KaiA is represented in pink, KaiC in blue, KaiB in orange, SasA in green, CikA in yellow, and RpaA in purple. The dark pink lines protruding from the CII subunit represent KaiC A-loops. The yellow and red stars represent the phosphosites S431 and T432, respectively. KaiB fold switch is represented on the left. RpaA phosphorylation is noted with a 'P' circled in red. The cycle progresses clockwise as depicted by the arrow drawn in the center.

Ch 1.2 THE FOLD SWITCH BEHAVIOR OF KaiB

KaiB is highly conserved among twelve cyanobacterial species and yet, the tetrameric structure adopts a fold that has not been previously reported [64]. The tetrameric form of KaiB has a negatively charged center, a positively charged perimeter, and aromatic ring zipper (fig. 1.3) [19]. KaiB is composed of two asymmetrical dimers (fig. 1.4A) [64]. Each dimer pair contains three α-helices covering half of the top and bottom and four β-sheets per subunit filling in the center [19]. The interface between the dimers consist of four aromatic residues one of which, Tyr^{94}, packs tightly against three consecutive prolines (P70, P71, P72) adding additional hydrophobic interactions that connect the dimers together [19].

The novel structure of tetrameric KaiB was baffling considering most sequence homologs have a thioredoxin and thiol-disulfide isomerase structure [19]. Recently, it was discovered that KaiB can also adopt a thioredoxin like fold, which is in fact the active form that sequesters KaiA (fig 1.4B) [9, 44]. In its inactive, or ground state (gs), conformation KaiB exist as dimer-of-dimers. However, when dissociated into monomeric units, KaiB switches into an active, or fold switch (fs), conformation. Ground state KaiB (gsKaiB) has a secondary structure of βαββααβ while fold switch KaiB (fsKaiB) has a secondary structure of βαβαββα (fig. 1.5) [9]. fsKaiB and gsKaiB exist in an equilibrium where fsKaiB is rare but, upon the phosphorylation of S431 fsKaiB is captured by CI, displacing SasA, and shifting the equilibrium towards fsKaiB [9]. The population shift from gsKaiB to fsKaiB is slow (hours timescale), allowing for the KaiC population to fully phosphorylate

under KaiA stimulation [9]. The fold switch behavior of KaiB allows it to sample two different conformations, classifying it as a new and rare metamorphic protein.

With only a handful of proteins identified as metamorphic [2], KaiB is currently the only one known to function in biological clocks. Under native conditions, metamorphic proteins can adopt different conformations for the same sequence thus contradicting the "one-sequence, one-fold paradigm" [2,3]. In the case of KaiB, the C-terminal half secondary structures (beginning with β3) completely switch (β to α and α to β). This large-scale secondary structure and oligomeric rearrangement points toward unfolding and refolding of the C-terminal half of KaiB. However, it is still unknown how KaiB dissociates and unfolds from a tetrameric βαββααβ fold to a monomeric βαβαββα fold.

Comparison of the gsKaiB and fsKaiB structures shows that three prolines undergo trans-to-cis isomerization. In the ground state conformation Pro^{63}, Pro^{70}, and Pro^{72} exist in a trans position and change to cis in the fold switch conformation (fig. 1.7). Proline isomerization exerts its functions through mechanisms involving (i) a conformational change caused by the 180° rotation about the prolyl bond, (ii) slow kinetics of isomerization providing a molecular timer, and/or (iii) recruitment of a prolyl *cis-trans* isomerase enzyme [80]. There have not been any identified *cis-trans* isomerase enzymes in the cyanobacterial clock system. However, the trans-cis isomerization behavior in KaiB does show a 180° rotation from its inactive to active state. Pro^{63} is located towards the N-terminal end of the α2 helix in gsKaiB and last residue in the coil prior to the β3 sheet in fsKaiB (fig 1.6). Likewise, Pro^{70} and Pro^{72} are at the N-terminal region of the α3 helices in gsKaiB but form a four residue long (Pro^{70}, Pro^{71}, Pro^{72}, Val^{73}) β-hairpin turn between β3 and β4 in fsKaiB

(fig 1.6). To elucidate the fold switching mechanism of KaiB, a good starting point is understanding the role of the prolyl trans-cis isomerization.

Here I describe the changes in thermo-stability of KaiB and several proline-to-alanine mutant variants. By mutating the proline residues to alanine, it is hypothesized that KaiB will be locked in the ground state conformation and thus become more stable. For information on the dynamics of wild-type KaiB and the proline-to-alanine mutants, NMR relaxation experiments were optimized using ubiquitin, a standard NMR test sample, to stress the importance of properly calibrating proton pulses and ionic strength concentrations in a protein sample.

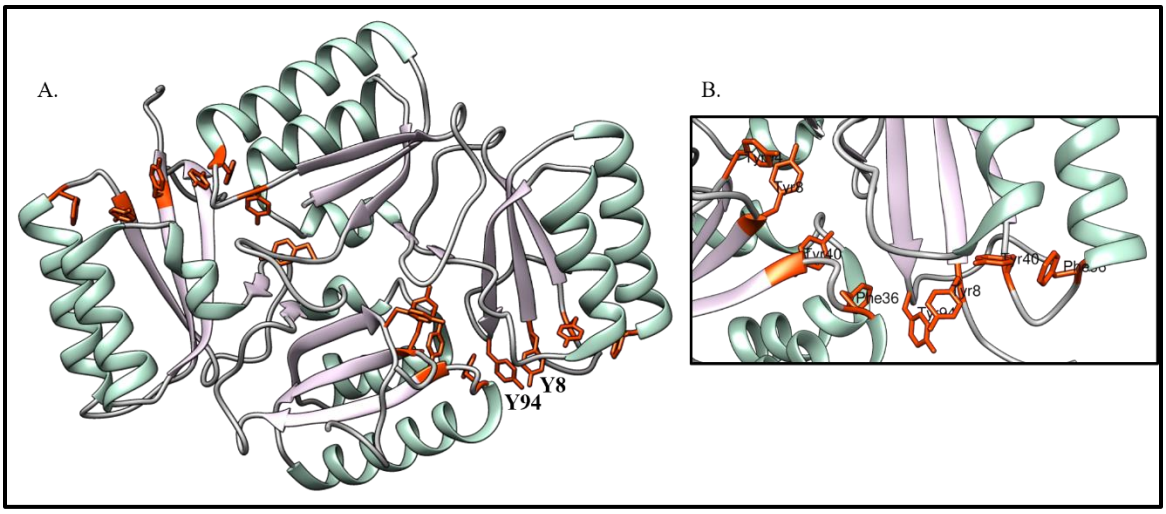

Figure 1.3: (A) Aromatic ring zipper is shown in red (Tyr^{8}, Phe^{36}, Tyr^{40}, Tyr^{94}). Residues Y8 and Y94 are labelled, a Y8A-Y94A substitution breaks the tetramer interface. (B) Closer look at the formation of the aromatic ring zipper.

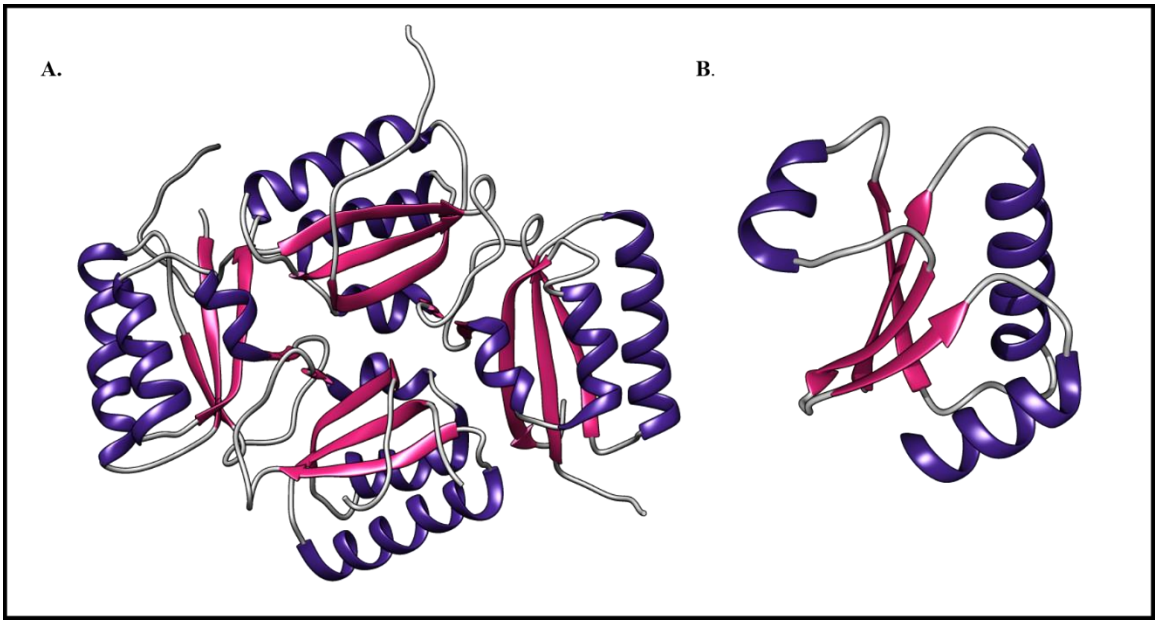

Figure 1.4: (A) Tetrameric gsKaiB. Secondary colors shown in pink (β-strands) and purple (α-helices). Coils are shown in gray. Tetrameric gsKaiB PDB 2QKE. (B) Monomeric fsKaiB with a thioredoxin-like fold. Structure obtained from LiWang lab (Chang 2015)

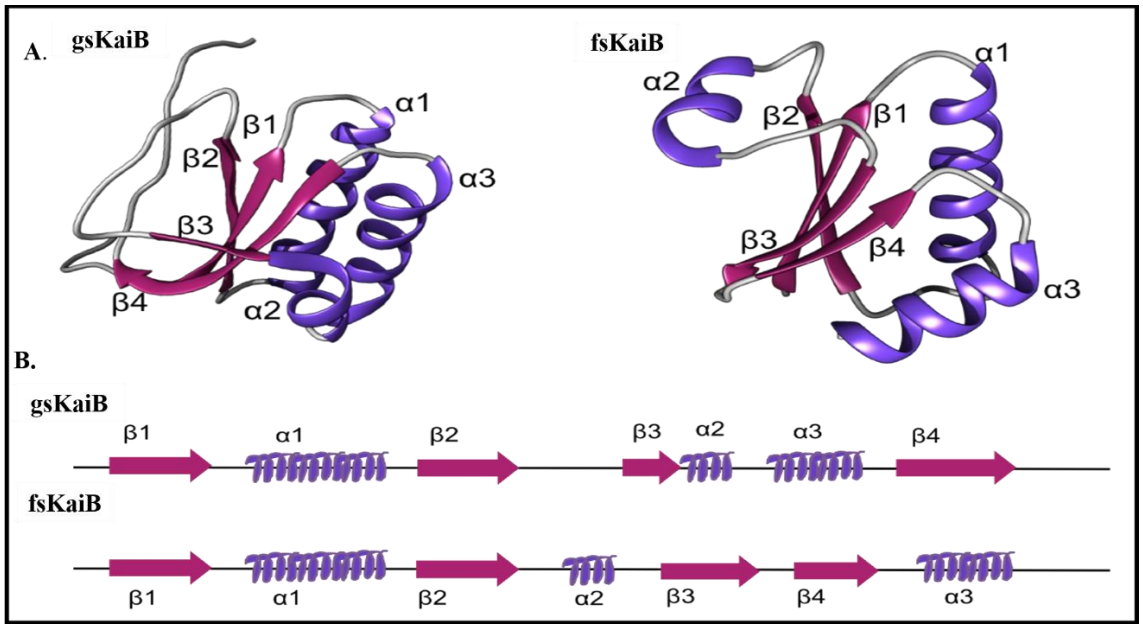

Figure 1.5: (A) Detailed tertiary structural comparison of a monomeric subunit of gsKaiB and fsKaiB (B) Secondary structural comparison of a monomeric subunit of gsKaiB (top) and fsKaiB (bottom). The N-terminal domain, $\beta 1$, $\alpha 1$, and $\beta 2$ remains the same while the C-terminal half, $\beta 3$, $\alpha 2$, $\alpha 3$, and $\beta 4$, in gsKaiB, change to $\alpha 2$, $\beta 3$, $\beta 4$, and $\alpha 3$ in fsKaiB.

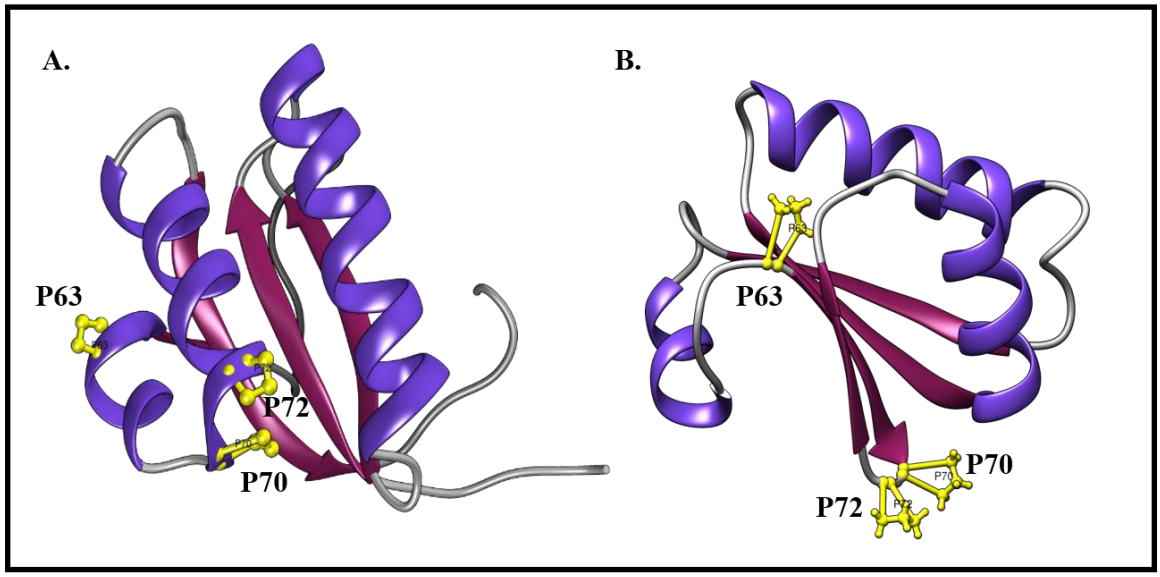

Figure 1.6: (A) gsKaiB proline residues 63, 70, and 72 highlighted in yellow. P63 is located on α2 and P70 and P72 are located on α3. (B) fsKaiB proline residues 63, 70, and 72 highlighted in yellow. P63 is located in the link between α2 and β3. P70 and P72 are in the β-hairpin between β3 and β4.

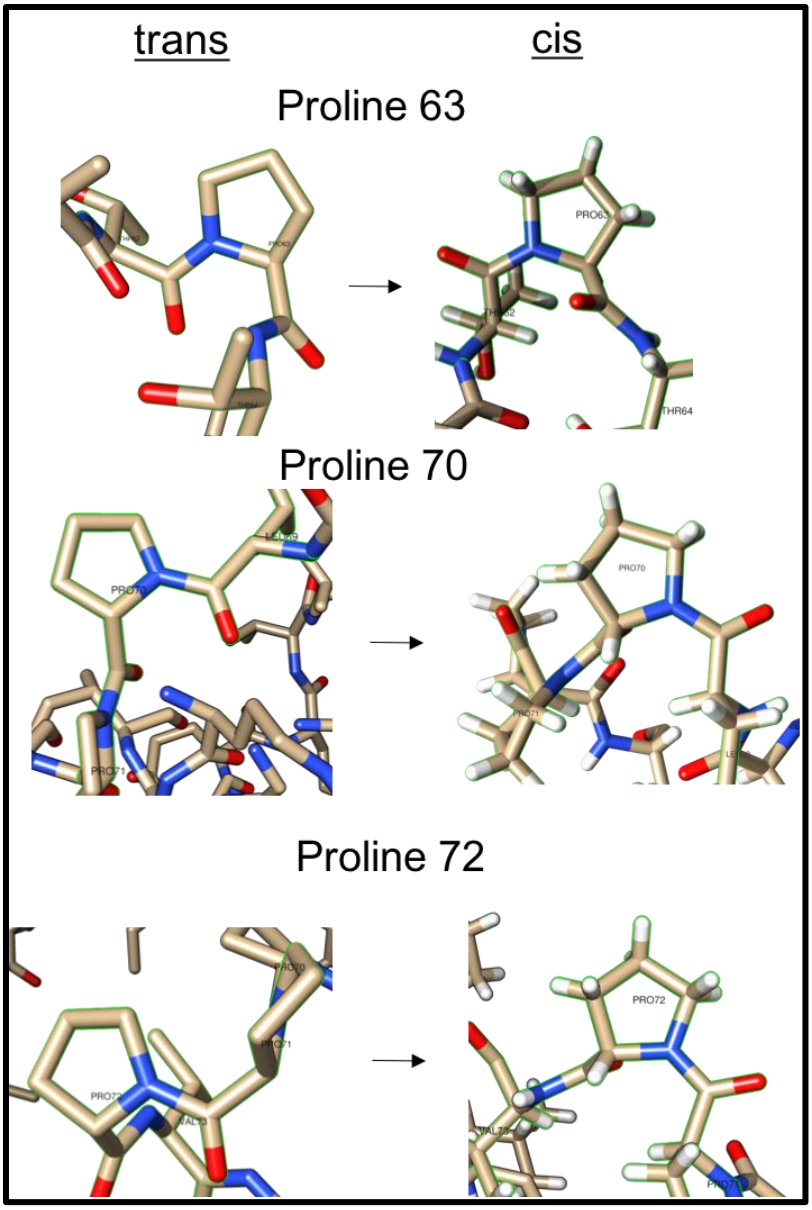

Figure 1.7: Trans-to-cis isomerase of proline 63, 70, and 72, respectively. Trans isomers are on the left (gsKaiB) and cis isomers are on the right (fsKaiB).

CHAPTER 2: TESTING THE THERMAL STABILITY OF KaiB

Ch 2.1 DIFFERENTIAL SCANNING CALORIMETRY

KaiB exists in equilibrium between ground state (gs) and fold switch (fs) conformations and therefore, is constantly in a partially 'unfolded' state as it samples the two folds. The goal of this study is to understand the contribution of the isomerization of three prolines to the fold switch behavior of KaiB. The hypothesis is that the flexibility of the C-terminal half would be restricted and thus locking KaiB in the gs conformation. To test this hypothesis, mutagenesis of the above prolines to alanine was performed and their stability as well as that of wild type KaiB was determined using differential scanning calorimetry (DSC). The rationale is that if KaiB is locked in the gs conformation its stability would be expected to increase as it is at the energy minimum.

The two-state system model was applied for this experiment. In a two-state system only the unfolded and folded (native) states are populated [26]. Although KaiB has at least three known states, (i) ground state, (ii) unfolded, and (iii) fold switch, the population of fsKaiB in a given sample is minimal and therefore, any contribution to the T_m or thermodynamic profile of the protein is negligible. This was determined by the A_w scaling factor. A_w is equivalent to the ratio $\Delta H_{cal}/\Delta H_{vH}$. If $\Delta H_{vH} > \Delta H_{cal}$ then the two-state system is valid; ΔH_{cal} is the calorimetric enthalpy given by the area under the transition peak and ΔH_{vH} is the calculated Van't Hoff enthalpy [57]. However, if $\Delta H_{vH} < \Delta H_{cal}$ (i.e. N⇔I⇔U) the two-state model is invalid [57]. All A_w values are less than 1 therefore, the two-state model can be applied (Table 2.1). The transition midpoint (T_m) between the

unfolded and native state is directly related to the stability of each protein [66]. By measuring the changes in the difference between the heat flow rate of the surroundings and the sample in a controlled environment, DSC can provide T_m and the change in heat capacity, enthalpy, and entropy [20].

Ch 2.2 MUTATIONS AND SAMPLE PREPARATION

Wild type gsKaiB exist in a tetrameric conformation. However, for this study, a truncated *Thermosynechococcus elongatus* KaiB dimer variant was used as the 'wild type' to facilitate NMR peak assignment. Each subunit of tetrameric KaiB contains four aromatic residues (Tyr^{8}, Phe^{36}, Tyr^{40}, Tyr^{96}) that align with the same aromatic residues of an adjoining molecule creating a zipper between the dimers (fig. 1.3) [(19)]. By mutating Tyr^{8} and Tyr^{94} to alanine, the aromatic zipper is destabilized creating a favored dimer structure. A C-terminus truncation at residue Asp^{99} was also included. Therefore, it is abbreviated as 'TBN99YY' and will be referred to as 'wild type KaiB'. Two-step polymerase chain reaction (PCR) was used to mutate Pro^{63}, Pro^{70}, and Pro^{72} to alanine individually and in combination. For primer sequences and two-step PCR protocol details refer to supplementary and methods, respectively. All proteins were expressed in LB and purified similarly (details in methods). Buffer choice for testing the thermodynamic stability of wild type (WT) KaiB and all mutant variants was 20mM potassium phosphate pH7.4. The pH of phosphate buffer remains relatively constant with changes in temperature thus reducing any possible effects of pH change on protein stability [(4)].

Nano differential scanning calorimeter (DSC) *TA Instruments* was used for all thermodynamic stability tests. All proteins were assayed under the same conditions; three heating cycles and two cooling cycles from 25℃ to 100℃, or vice versa, at a rate of $1℃/min$. Artifacts due to air bubbles were eliminated by running multiple cycles. For details on the program or sample set up please see methods.

Ch 2.3 TRANSITION MIDPOINT COMPARISON OF WT KaiB AND PROLINE MUTANT VARIANTS

WT KaiB showed a transition midpoint (T_m) equal to 72.9 $\pm$0.01℃. Although KaiB mutants were hypothesized to have higher T_m values, some mutants showed similar or lower T_m values than that of WT KaiB, suggesting their differential roles in KaiB fold switching. A comparison of all the T_m values are listed in Table 2.1. When individually mutated to alanine, P63A and P72A KaiB mutants had similar values as wild type KaiB. P63A showed a very minimal difference (0.1 ± 0.02℃) in T_m value while P72A showed a slightly more noticeable decrease in stability (1.5 ± 0.01℃) T_m. This indicates that P72A is slightly less stable than WT KaiB. However, the differences in T_m between wild type KaiB and P63A are negligible. Therefore, it can be concluded that the stability of P63A KaiB is similar to that of wild type KaiB. On the other hand, P70A has a $T_m = 52.4 \pm 0.03$ ℃, a 20.49 difference in T_m from wild type KaiB.

Combinations of proline to alanine mutants were also tested and showed a similar trend to that of the individual mutants. Double mutant P63A-P70A and triple mutant P63A-P70A-P72A also had T_m values comparable to P70A, 55.8 ± 0.03℃ and 50.5 ± 0.3℃, respectively. Double mutant P63A-P72A KaiB had a T_m value equal to 75.28 ± 0.05℃. Therefore, when mutations P63A and P72A are combined, they stabilize KaiB more over wild type KaiB. However, the stability of KaiB is drastically reduced when mutant P70A is introduced. Interestingly, when P63A, the most stable among the single mutant variants, is introduced to P70A-P72A to create the triple mutant, it is even further destabilized. A KaiB P70A-P72A construct was also made but the thermodynamic stability was not

determined because it could not be purified and requires further study to optimize purification. This indicates the likelihood that mutant P70A-P72A is the least stable. Therefore, residue Pro^{70} in gsKaiB is critical for protein stability.

Change in entropy was also calculated using the *Gibbs equation,* $\Delta G = \Delta H - T\Delta S$ (eq. 2.1). At the melting temperature $\Delta G_m = 0$, therefore equation 2.1 can be rearranged as $\Delta S_m = \frac{\Delta H_m}{T_m}$ (eq. 2.2) where T_m is the transition midpoint (table 2.1) [(5)]. WT KaiB has the highest ΔS_m (2.2 ± 0.04 kJ/(mol·K)) indicating a greater increase of disorder at T_m [(70)]. The three of most stable KaiB mutants P63A ($\Delta S_m = 1.8 \pm 0.06$ kJ/(mol·K)), P63A-P72A ($\Delta S_m = 1.8 \pm 0.05$ kJ/(mol·K)), and P72A ($\Delta S_m = 1.7 \pm 0.04$ kJ/(mol·K)) had lower ΔS_m values. However, mutants containing P70A had the lowest ΔS_m values; P70A ($\Delta S_m = 1.3 \pm 0.04$ kJ/(mol·K)), P63A-P70A ($\Delta S_m = 1.5 \pm 0.04$ kJ/(mol·K)), and P63A-P70A-P72A ($\Delta S_m = 1.1 \pm 0.17$ kJ/(mol·K)). Therefore, the less stable a KaiB mutant, the more "unfolded" it already is. I.e. KaiB mutants are already disordered to some extent and unfolding them completely does not result in a large increase in disorder. Although this data suggests that the proline to alanine mutant KaiB variants have a smaller increase of disorder at T_m, the baseline in the raw data has a negative slope (supplementary). After the protein is melted the change in heat capacity should increase and have a positive slope [(16)]. This could have an effect on the measure ΔH (area under the curve) therefore, these values are tentative.

Proline residues tend to destabilize alpha helices by bonding to the backbone of the protein and disrupting the H-bond network [(6)]. Typically, a proline can fit well into the first turn of an alpha helix without causing major steric hindrance by eliminating the backbone

amide-proton bond [6]. All three proline residues, Pro^{63}, Pro^{70}, and Pro^{72}, are located in the first turn of an alpha helix. However, alanine has a high helix propensity and is a 'good α-helix former' [6, 52]. Therefore, it was unexpected that replacing a proline residue with an alanine would destabilize KaiB. In gsKaiB both Pro^{63} and Pro^{72} are the third residues from the N-terminal of α2 and α3, respectively. Whereas Pro^{70} is the first residue of the α3 helix. The location of these prolines may help explain why the switch from proline to alanine at Pro^{63} or Pro^{72} has little to no change in stability and opposite effects are seen at Pro^{70}.

In addition to being the first residue of the α3 helix in gsKaiB, Pro^{70} is also the first residue in the β hairpin connecting β3 and β4 in fsKaiB. Therefore, it is possible that Pro^{70} acts as a 'molecular hinge' introducing bending/kink-swivel motions necessary for protein stability [7]. Size exclusion data also points to differences in overall size of each mutant variant compared to WT KaiB. Nearly all of the KaiB mutants eluted at or after the elution volume of WT KaiB, except for P63A-P72A. Double mutant P63A-P72A is the most sable KaiB variant ($T_m = 75.28$℃) but also elutes before WT KaiB, indicating a larger size. Table 2.2 list the elution volumes of all the protein variants. Although DSC and size exclusion chromatography can respectively provide information on the stability and relative size of proteins, they do not provide information on protein dynamics. Therefore, NMR relaxation experiments will be used in the future to obtain detailed information on the global and local behavior of KaiB.

Protein	T_m (℃)	ΔH_m (kJ/mol)	ΔS_m (KJ/(mol·K))	A_w
TBN99YY	72.9 ±0.01	744.0 ±5.1	2.2 ±0.04	0.040
TBN99YY-P63A	72.8 ±0.03	637.6 ±5.1	1.8 ±0.06	0.053
TBN99YY-P70A	52.4 ±0.03	421.9±4.1	1.3±0.04	0.060
TBN99YY-P72A	71.4 ±0.02	588.0±3.9	1.7±0.04	0.045
TBN99YY-P63A-P70A	55.8±0.03	493.5±8.3	1.5±0.04	0.057
TBN99YY-P63A-P72A	75.3±0.05	642.5±8.8	1.8±0.05	0.018
TBN99YY-P63A-P70A-P72A	50.5±0.30	350.7±23.2	1.1±0.17	0.046
TBN99YY-P70A-P72A	NA	NA	NA	NA

Table 2.1: Table listing WT KaiB (TBN99YY) and proline to alanine mutants. Data for TBN99YY-P70A-P72A was not available. A_w is the scaling factor. T_m and ΔH_m were derived from the *TA Instruments Launch NanoAnalyze* modeling software. ΔS_m values were calculated based on the T_m and ΔH_m (equation 2.2). A 95% confidence level was applied to all models. Aw confidence interval was negligible and therefore not included.

Protein	Elution Volume (mL)
TBN99YY	74
TBN99YY-P63A	75
TBN99YY-P70A	75
TBN99YY-P72A	75
TBN99YY-P63A-P70A	74
TBN99YY-P63A-P72A	72
TBN99YY-P63A-P70A-P72A	74
TBN99YY-P70A-P72A	NA

Table 2.2: Elution volume based on size exclusion chromatography for WT KaiB and proline to alanine mutants. Column used: HiLoad™ 16/600 Superdex™ 75pg.

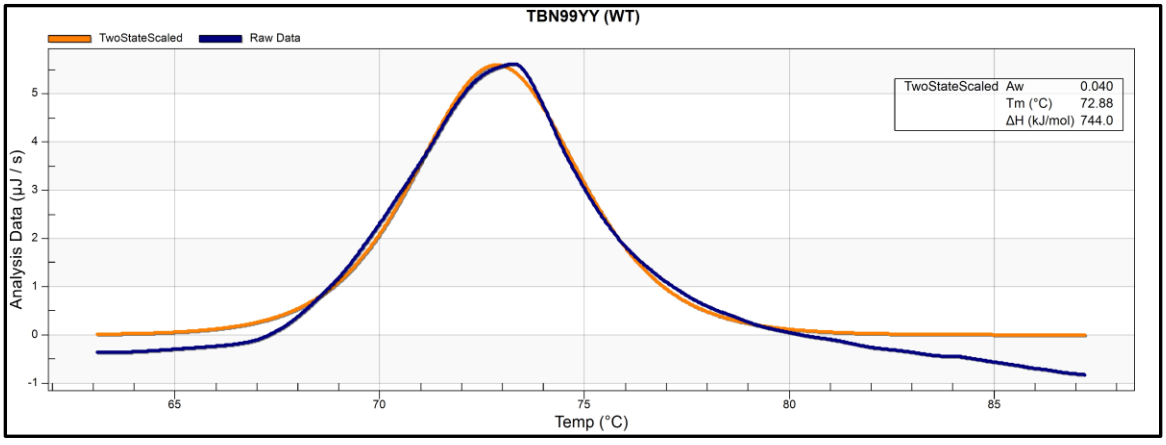

Graph 2.1: WT KaiB (TBN99YY) DSC data. Two State Scaled model in orange. Raw data is in blue. Y-axia is heat capacity. X-axis is temperature. Full thermodynamic profile from 25℃ to 100℃ can be found in supplementary.

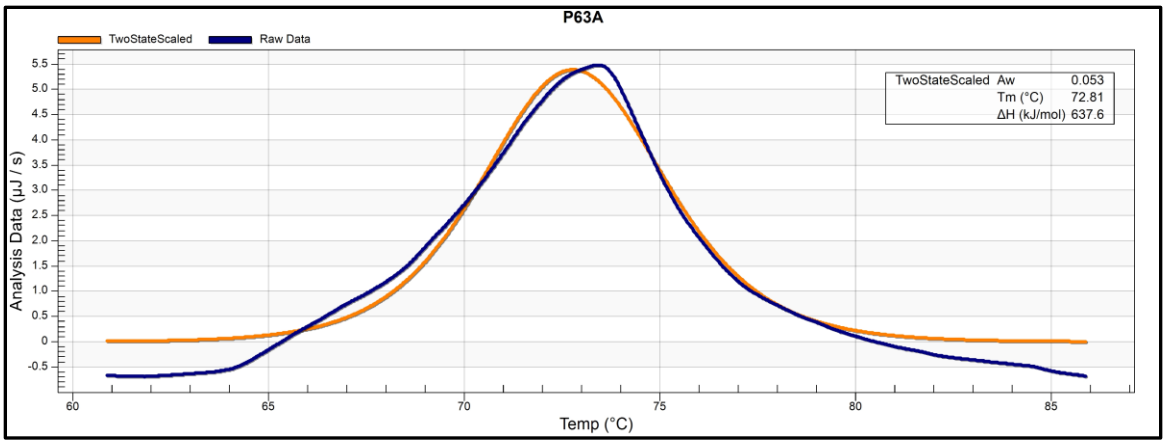

Graph 2.2: TBN99YY-P63A DSC data. Two State Scaled model in orange. Raw data is in blue.

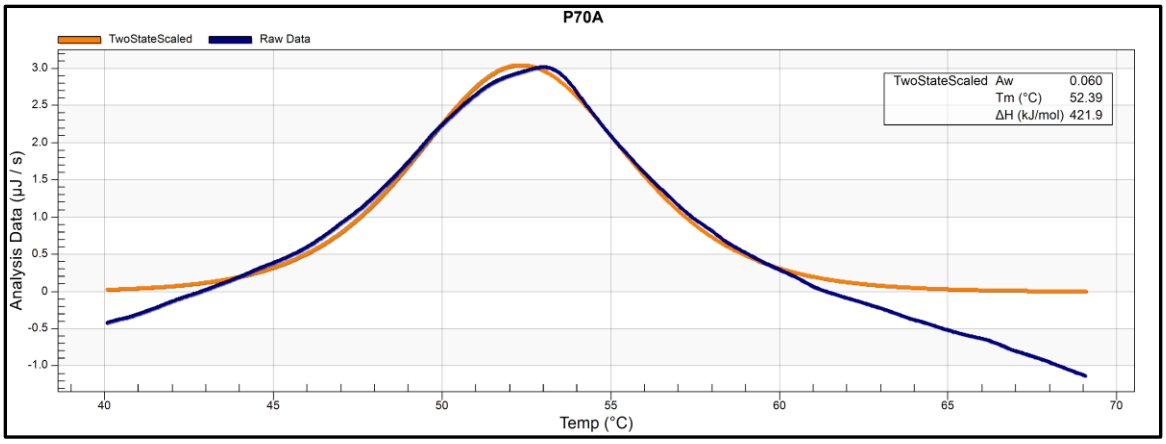

Graph 2.3: TBN99YY-P70A DSC data. Two State Scaled model in orange. Raw data is in blue.

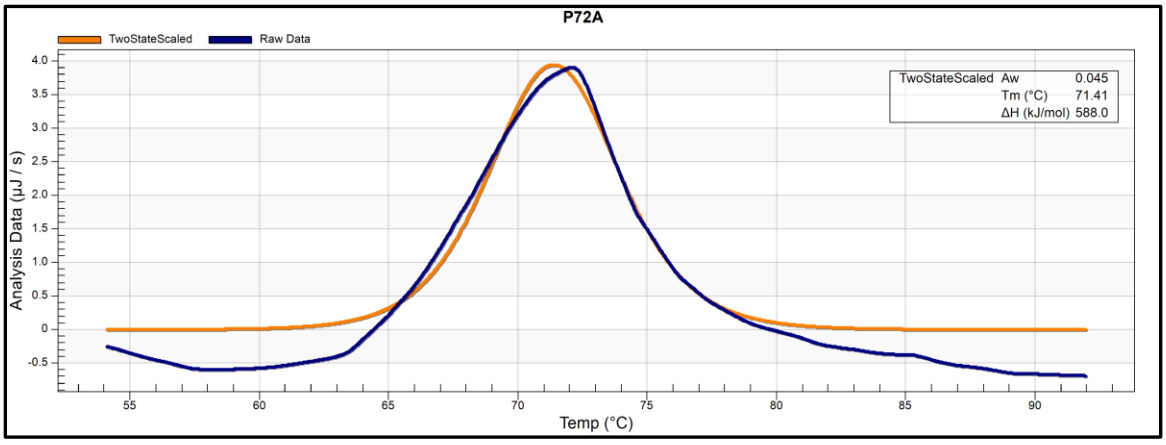

Graph 2.4: TBN99YY-P72A DSC data. Two State Scaled model in orange. Raw data is in blue.

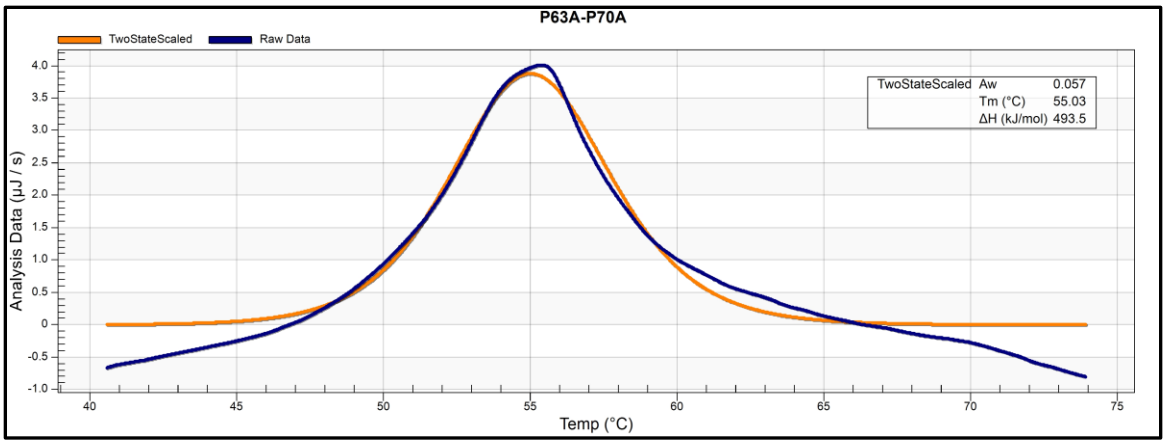

Graph 2.5: TBN99YY-P63A-P70A DSC data. Two State Scaled model in orange. Raw data is in blue.

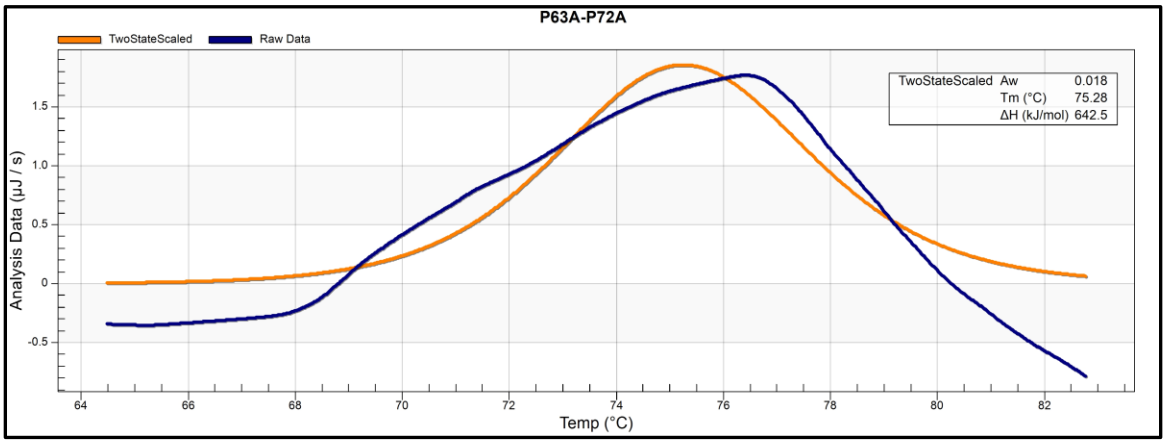

Graph 2.6: TBN99YY-P63A-P72A DSC data. Two State Scaled model in orange. Raw data is in blue. An unusually broad peak is shown. It is possible that a population of the protein may be missfolded resulting in a broad melting range.

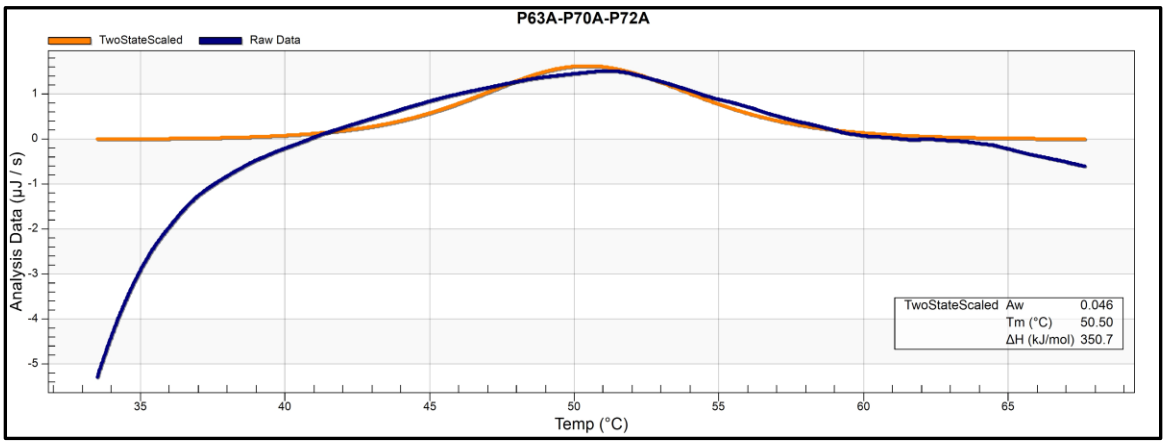

Graph 2.7: TBN99YY-P63A-P70A-P72A DSC data. Two State Scaled model in orange. Raw data is in blue. Similar to P63A-P72A, a brad peak is also shown. This may be caused by a missfolded protein population.

CHAPTER 3: THE IMPORTANCE OF PROPERLY CALIBRATING ^{1}H PULSES FOR MEASURING ^{15}N T_1 RELAXATION TIME

Ch. 3.1 ^{15}N T_1 RELAXATION

All proteins contain varying degrees of flexibility within their tertiary fold [3]. NMR relaxation experiments can examine these internal dynamics and provide detailed information pertaining to these fluctuations [32]. Relaxation studies also have the advantage of probing the backbone dynamics of a protein on a per residue basis on the millisecond to second time scale [34, 31]. Relaxation studies typically encompass ^{15}N T_1, T_2, and ^{15}N{-H} Nuclear Overhauser Effect (NOE) experiments that map out the spectral density functions that describe protein motions at a number of frequencies [31]. In a metamorphic protein, such as KaiB, understanding the local motility could bring insight into how it can exchange between two conformations under native conditions. More specifically, Nuclear Magnetic Relaxation (NMR) relaxation has the potential to identify the role of trans/cis isomerization of the three prolyl residues (p63, P70, P72) in KaiB fold switching.

NMR relaxation is the process that allows a system to regain thermal equilibrium, a process described by the Boltzmann distribution, i.e. as the energy of a particular state of the surroundings increase, the probability of that state being occupied decreases [41,34]. Typically, relaxation is divided into two types; *transverse relaxation* (spin-spin relaxation) and *longitudinal relaxation* (spin-lattice relaxation) [41]. Relaxation causes transverse magnetization to reach an equilibrium value of zero and longitudinal magnetization to return the *Z*-magnetization to equilibrium [34]. The *Z*-magnetization at equilibrium is

proportional to the population difference between α and β energy levels [34]. In this chapter the focus will be on longitudinal relaxation. Longitudinal, or spin-lattice, relaxation is the exchange of energy between spins fluctuating magnetic fields that are resonant with the spins. The molecular motions are the energy reservoir or 'lattice' [34]. Therefore, longitudinal relaxation is described as a result from the transitions between the α and β energy levels [41]. Longitudinal relaxation is characterized by the first-order rate expression $\frac{dM_z(t)}{dt} = -R_1[M_z(t) - M_z^0]$ where M_z represents *Z*-magnetization and R_1 the rate constant [34, 71]. One over the rate constant R_1 is equal to T_1, $T_1 = {}^1/_{R_1}$, which is the exponential time constant of the system returning to thermal equilibrium [34, 71]. Time required for a population to return to equilibrium form the transverse (*xy)* plane is system specific; systems with slower T_2 relaxation have a longer T_1 and vice versa [34, 41].

Relevant to protein dynamics, T_1 relaxation depends on the spectral density at the Larmor frequency [71]. The spectral density is the Fourier transform of the correlation function [34]. The correlation function characterizes the time dependence of the random motions of a sample by averaging the time it takes a molecule to move approximately one radian from its starting position [34]. Therefore, we can use T_1 relaxation rates to find information on the molecular motions of proteins on a per residue bases.

Ch. 3.2 SAMPLE CONDITIONS AND PREPARATION

Before beginning relaxation experiments on KaiB and the KaiB mutant variants, a control, Ubiquitin (pET-11a-Ubiquitin Amp^+), was used to establish accurate T_1 relaxation measurements. Ubiquitin is a highly soluble, stable, well characterized protein with published T_1 relaxation values [68, 77]. The T_1 relaxation values measured here were compared to those calculated in 1995 by Tjandra et al. In accordance with Tjandra et al. the sample conditions were set as follows; 1.4mM, pH 4.7, 10mM NaCl, at 27℃ [77]. These parameters remained the same for all experiments. For ^{15}N protein expression, purification, titration, and buffer preparation, please see methods. A 5mm BMS-3 Shigemi D_2O matched symmetrical microtube ('Shigemi tube') was used for all experiments and ran on a Bruker 600 MHz AVANCE III spectrometer equipped with a TCI cryoprobe and z-axis pulsed-field gradient capability. Shigemi tubes have a 10 mm plug of susceptibility matched glass at the bottom of the tube and an equivalent to cover the top of the sample in the form of a plunger, reducing the sample volume needed by matching the susceptible volume required for the receiver coil of the probe [49]. The purpose of the glass plugs is to eliminate any change in magnetic susceptibility of the solvent/glass interface [49]. Shigemi tubes also provide better sample stability due to reduced air oxidation and more favorable shimming and water suppression. Thus, providing a better spectrum with diminished water ^1H signals.

Ch. 3.3 EFFECTS OF ^{1}H PULSE CALIBRATION ON ^{15}N T_1 RELAXATION

Water protons have a relatively long T_1 relaxation time (4-5 seconds) compared to that of protein protons (~1.4 seconds) therefore, water protons remain partially saturated between pulses [17]. For signal-to-noise purposes, it is necessary in NMR experiments for the repetition rate per scan to be faster than the relaxation rate of bulk water, resulting in semi-saturated water protons [33]. The semi-saturated water protons can then replace amide protons via chemical exchange [33], leading to longer T_1 times for protein protons [43]. In ^{15}N T_1relaxation experiments, $^{1}H^{N}$ are decoupled during the ^{15}N relaxation delay. Thus, longer relaxation delays can lead to more severe H_2O saturation and thereby artificially weaker $^{1}H^{N}$ signals that manifest as apparently shorter ^{15}N T_1 times [40].

During the first trial of measuring T_1values for the ubiquitin control sample, ^{1}H pulses were calibrated using the Bruker PulseCal program. The Bruker PulseCal program nutates water protons about an applied field during the free-induction decay (FID) [85]. When comparing the results of the pulse calibration methods to those acquired by Tjandra *et al.*, Tjandra's 1995 sample had longer ^{15}N T_1 values than those acquired using ^{1}H pulses calibrated using PulseCal (Graph 3.1). Graph 3.1 shows Tjandra's T_1 values (nicoT1a:1995 data) versus the T_1values after a PulseCal program (exp400:T1N15_rk.nl, pulsecal) with a relaxation delay of D1=1.5s. Purple outlined circles indicate the correlation between experiments for each residue. The green dashed line is along the diagonal. As shown in graph 3.1, the diagonal is below the residue population informing that the T_1 values for ^{1}H PulseCal program of the ubiquitin sample are slightly shorter, rmsd=0.027sec. Because

both samples were prepared and ran under similar conditions, these results hinted toward a discrepancy in the pulse calibration method.

Suggested by Jinfa Ying at the NIH (through personal contact), a new pulse calibration method of minimizing the first point of the FID after a 180° ^{1}H pulse was tested. Graph 3.2 shows a comparison between the new "Jinfa-style" (exp402(T1N15_rk.nl)) versus the Bruker ^{1}H PulseCal method (exp400(T1N15_rk.nl)). The PulseCal method had dramatically shorter ^{15}N T_1 values, rmsd=0.101sec. As mentioned previously, shorter ^{15}N T_1 can be due to inadvertent water saturation during ^{15}N relaxation delays [40].

The ^{15}N T_1values for the ubiquitin control sample were measured again using the "Jinfa-style" ^{1}H pulse calibration method. To confirm if there is an advantage to the "Jinfa-style" ^{1}H pulse calibration method, it was compared to Tjandra's 1995 method (Graph 3.3). With a relaxation delay of D1=1s, the "Jinfa-style" ^{1}H pulse calibration (exp404(T1N15_rk.nl,2017) method showed to have longer T_1 relaxation values relative to Tjandra's 1995 ^{1}H pulse calibration method (nicoT1a(1995)), rmsd=0.088sec. These results verify that properly calibrating ^{1}H pulses is directly linked to accurately establishing T_1 relaxation values. In addition, these results highlight the importance of artificially minimizing T_1values as a result from chemical exchange between saturated water protons and amide protons.

Lastly, the new "Jinfa-style" ^{1}H pulse calibration method was tested against different recycle delay times (Graph 3.4). The recycle delay is the time between scans to allow *Z*-magnetization to return to a fraction of its thermal equilibrium value and is determined by the T_1 relaxation times [34]. Three second (exp403(T1N15_rk.nl)) and one

second (exp404(T115N_rk.nl)) recycle delay times were tested. Set up with identical ^{1}H pulse calibration methods, recycle delay time had little to no effect on the T_1 values, rmsd=0.006sec (graph 3.4). These results further confirm that properly calibrating ^{1}H pulses yield the most accurate and reliable ^{15}N T_1 values independent of relaxation delay times.

The "Jinfa-style" ^{1}H pulse calibration methods yields longer ^{15}N T_1 values because it more accurately calibrates the flip angle of pulses on water, leading to better water suppression compared to the PulseCal program. For NMR relaxation studies of WT KaiB and the proline to alanine mutant variants, accurately measuring T_1 values is crucial in being able to identify any local and global changes. Thus, properly calibrating ^{1}H pulses is an important step in identifying ^{15}N T_1 relaxation values.

Equation 3.1: Root mean square deviation [38]

$$RMSD = \sqrt{\frac{1}{n}\sum_{i=1}^{n} d_i^2}$$

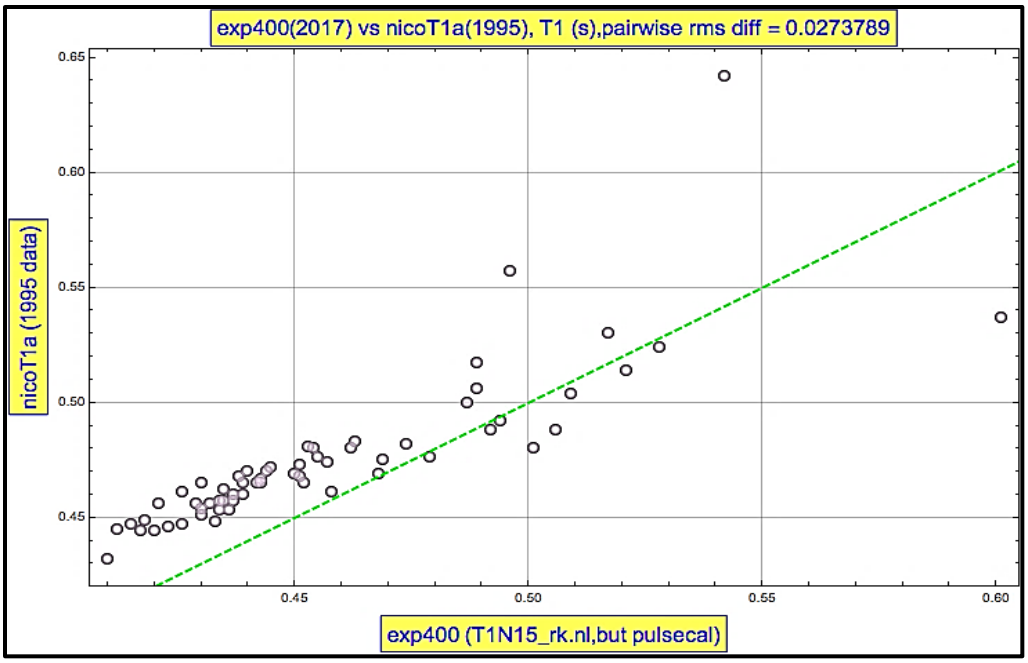

Graph 3.1: X-axis, exp400(T1N15_rk.nl), represents the T_1 values calculated using the PulseCal program. Y-axis, nicoT1a, represents the T_1 values obtained from Tjandra *et al.* 1995. T_1 values from PulseCal are shorter than Tjandra *et al* 1995 data. Purple outlined circles indicate the correlation between experiments for each residue. The green dashed line represents the diagonal. D1 is the recycle delay. Units are in seconds. rmsd=0.027sec.

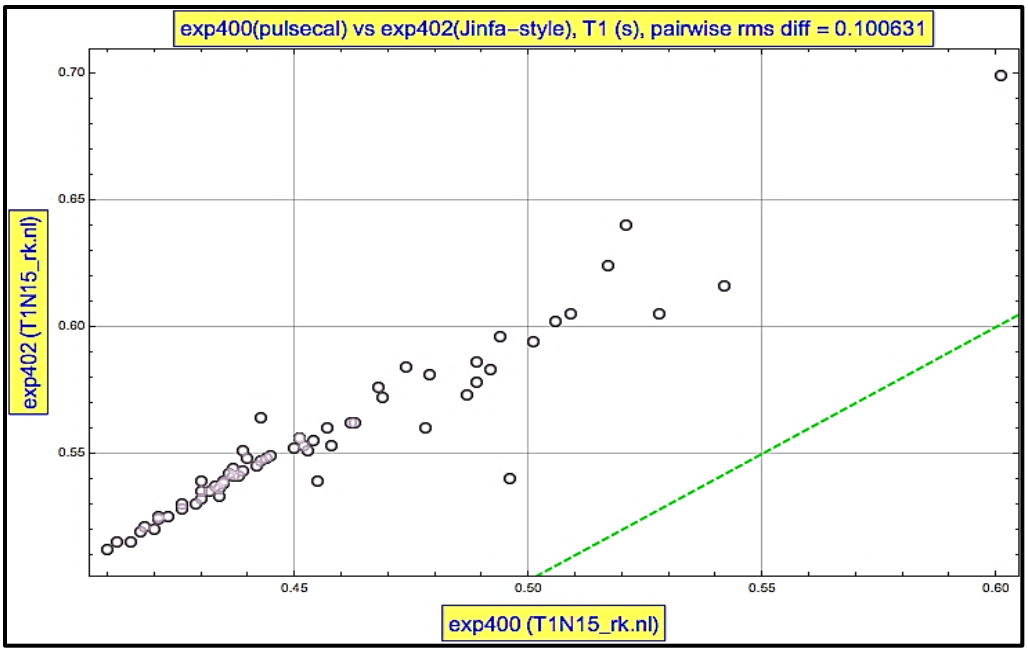

Graph 3.2: X-axis, exp400(T1N15_rk.nl), represents the T_1 values calculated using the PulseCal program. Y-axis, exp402(T1N15_rk.nl), represents the T_1 values calculated using the "Jinga-style" ^{1}H calibration method. The PulseCal methods showed significantly shorter T_1 values. rmsd= 0.101sec.

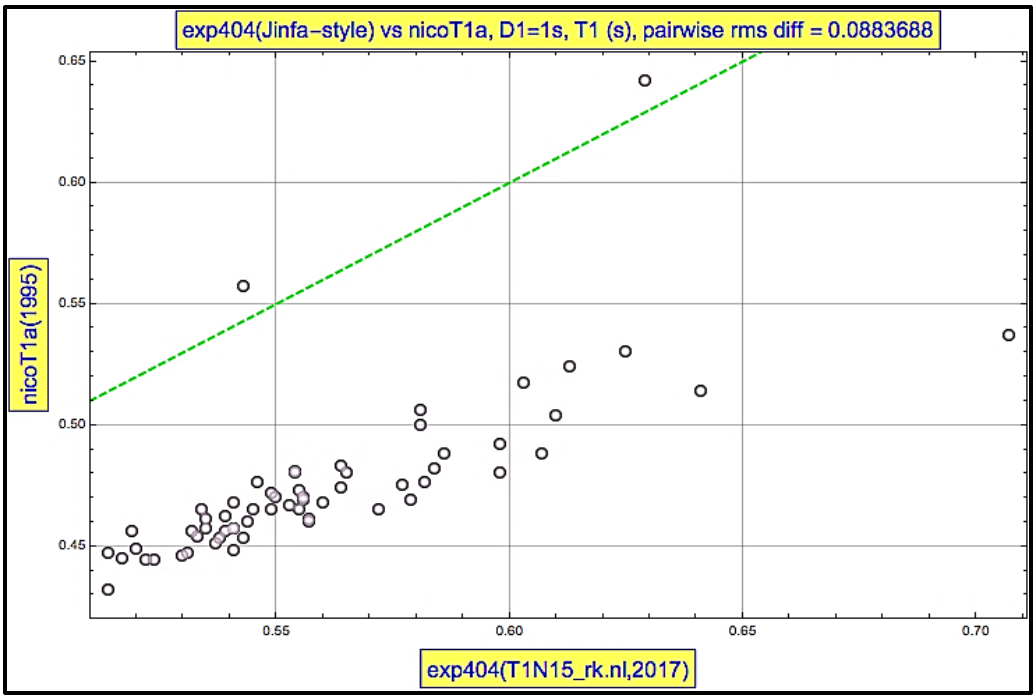

Graph 3.3: X-axis, exp404(T1N15_rk.nl,2017), represents the T_1 values calculated using the "Jinfa-style" ^{1}H calibration methods. Y-axis, nicoT1a(1995), represents the T_1 values calculated using Tjandra *et al* ^{1}H pulse calibration methods. The "Jinfa-style" ^{1}H calibration produces longer T_1 values than the method used by Tjandra *et al*, 1995. rmsd=0.088sec.

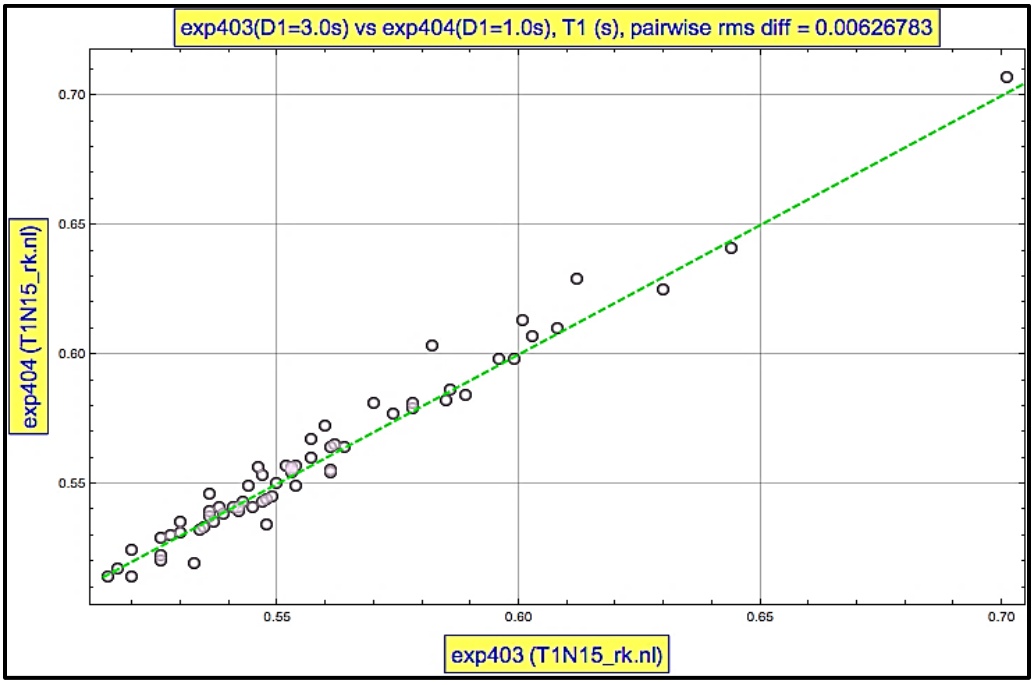

Graph 3.4: Both experiments were calculated using the "Jinfa-style" ^{1}H calibration method but with different recycle delay times. Exp403(T1N15_rk.nl), x-axis, D1=3s. Exp404(T1N15_rk.nl), y-axis, D1=1s. rmsd= 0.006sec.

Ch. 3.4 EFFECTS OF IONIC STRENGTH ON ^{15}N T_1 RELAXATION

Ion concentration in protein samples can help maintain the protein in a soluble state. Typically, as ionic concentration (or strength) increases so does the solubility of the protein along with its secondary and tertiary structures [61]. The ion concentration needed to keep a protein of interest soluble is sample specific but generally follows the Hofmeister series [12]. The Hofmeister series classifies ions based on their ability to "salt-out" or "salt-in" proteins and therefore affect protein stability [4]. Ubiquitin, a highly charged thermostable globular protein, is both soluble and stable at a low salt concentration [21,77]. For the study described here, a 10mM NaCl buffer was used and titrated to different ion concentration while maintaining a pH of 4.7.

Two ubiquitin samples, "High Salt" and "Low Salt", were prepared to study the effects of ionic strength. Both samples were prepared similarly with the exception of the final step. For details on purification and expression, refer to methods. The "High Salt" (HS) sample underwent buffer exchange after size exclusion chromatography with a 10 mM NaCl solution without titration. After buffer exchange the HS sample was concentrated to a 1.5 mM stock solution. After preparation of the HS NMR sample, 1.4mM Ubiquitin, 5% D_2O, 0.02% NaN_3, 20μM DSS, 1x Protease Inhibitor, the sample was titrated to pH 4.7 with 1M NaOH and 0.5M NaCl, the final ionic strength was calculated to be 44.8 mM. The "Low salt" (LS) sample was prepared by buffer exchange with a pre-titrated 1L pH 4.7 10mM NaCl solution. The final ionic strength of the LS sample was calculated to be 10.01 mM.

At high ionic strength, dielectric effects can lower the NMR signal-to-noise ratio and thereby increase acquisition times [49]. Dielectric compounds, such as NaCl, are electrical insulators that can be polarized by an applied electric field [54]. Thus, as ionic strength in a solution increases the more electromagnetically insulated a sample becomes, making it impossible to achieve uniform 90° flip angle across the width of the sample [61]. Non-uniform ^{1}H flip angles lead to water saturation and, as mentioned previously, can cause artificially low ^{15}N T_1 values [17]. As shown in graph 3.5, the HS sample (exp401 (high salt)) has an abnormally low T_1 value, rmsd=0.041sec. Both samples were calibrated using the "Jinfa-style" ^{1}H pulse calibration method and had a relaxation delay of D1=1.5. This exercise demonstrates the difficulty of properly suppressing water in high salt samples. Therefore, NMR relaxation experiments of WT KaiB and the proline to alanine mutants should be prepared in a low ionic strength buffer.

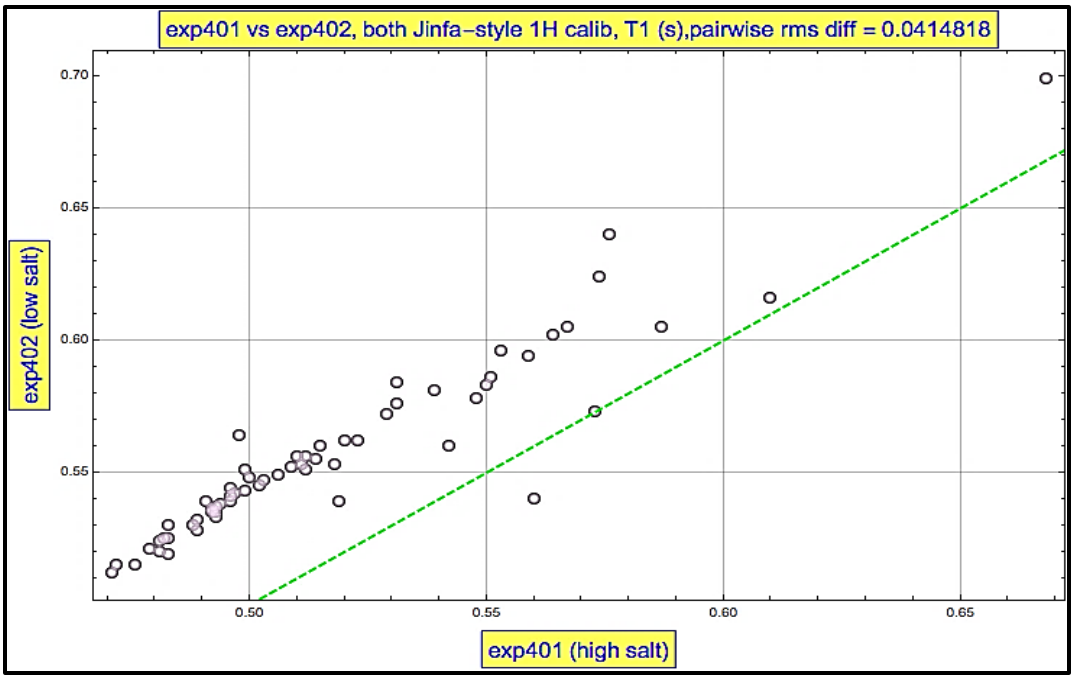

Graph 3.5: Both experiments were calibrated using the "Jinfa-style" method. The high salt sample, exp401, shows lower T_1 values than the low salt, exp402, sample. rmsd=0.041sec.

CHAPTER 4: SUMMARY AND DISCUSSION

Circadian clocks are found in animals, plants, fungi, and bacteria. Three main characteristics are shared among all circadian clocks: (1) temperature compensation, (2) phase resetting, and (3) an endogenous, near 24-hour cycle [14]. To begin to understand how circadian clocks function it is necessary to understand the underlying molecular mechanisms governing the 24-hour cycle. The circadian clock of cyanobacteria is ideal for such mechanistic studies because it is the most simplistic system known [9]. Consisting of only three core oscillator proteins, KaiA, KaiB, and KaiC, the cyanobacterium circadian clock can be reconstituted *in vitro* by the addition of its three components. The heart of the oscillator, KaiC, has kinase and phosphatase activities that generate the 24-hour phosphorylation rhythm under regulation of KaiA and KaiB [73]. KaiC, a double-donut shaped hexamer, has two homologous domains, CI and CII [56]. Phosphorylation sites of KaiC, S431 and T432, are located on the CII domain [50]. The cycle of KaiC autophosphorylation proceeds as follows, ST →SpT→ pSpT → pST → ST [89, 90]. When S431 is not phosphorylated, KaiA stabilizes the exposed A-loops on the CII domain promoting autokinase activity of KaiC [78]. Concomitantly, output protein SasA can freely bind to the B-loops on the CI domain of KaiC, activating phosphorylation of transcription factor and response regulator RpaA [23, 81, 51]. Upon phosphorylation of S431, the CII ring tightens, exposing the KaiB binding cite on CI [87]. KaiB and N-terminal SasA are homologous and bind to the same location on KaiC [10]. KaiB can outcompete SasA for B-loop binding on CI [78]. While bound to CI, KaiB also sequesters KaiA and interacts with output protein CikA, whereupon CikA dephosphorylates RpaA (fig. 1.2) [67, 18, 87].

Among the three components of the Kai clock, KaiB, possess a distinct feature found only in a handful (~10) of proteins; it is metamorphic [2, 9]. Before KaiB can bind the B-loops on CI, it must first switch folds from an inactive (ground state) conformation to an active (fold switch) conformation [9]. Ground state (gs) KaiB is a dimer of dimers with a βαββαaβ fold, while fold switch (fs) KaiB is a monomer with a thioredoxin-like fold (βαβαββα) (fig 1.5) [19, 9]. Comparison of these two structures shows three proline residues, Pro^{63}, Pro^{70}, Pro^{72}, that undergo a trans to cis isomerization. Studying the trans-cis isomerization can elucidate the fold switching mechanism of KaiB. I have mutated Pro^{63}, Pro^{70}, and Pro^{72} to alanine individually and in combinations. The hypothesis is that without the ability to undergo a trans-cis isomerization KaiB will be locked in its ground state conformation thus increasing stability. Differential Scanning Calorimetry (DSC) and Nuclear Magnetic Resonance relaxation experiments were employed to test this hypothesis. The information derived from these experiments can provide 'snapshots' of the protein stability of KaiB as fold switching is restricted.

DSC experiments using the two-state system model were used to calculate the transition midpoint, T_m, of wild type (WT) KaiB and the proline-to-alanine mutant variants. Proline-to-alanine mutations at residues 63 and 72 individually have similar T_m values, 72.8±0.03℃ and 71.4±0.02℃, respectfully, as WT KaiB (72.9±0.01℃). However, when combined (P63A-P72A), KaiB becomes more stable (T_m =75.3±0.05℃). In contrast, a mutation introduced at proline residue 70 drastically reduces the transition midpoint indicating a decrease in stability; T_m for P70 is 52.4±0.03℃, 55.8±0.03℃ for P63A-P70A, and 50.5±0.30℃ for P63A-P70A-P72A. Both Pro^{63} and Pro^{72} are the third residues from

N-terminus of the α2 and α3 helices while Pro^{70} is the first residue of the α3 helix. The position of Pro^{70} suggest that it may act as a 'molecular hinge' that introduces bending/kink-swivel motions required for protein stability [7].

In a study conducted by Miller *et al*, they identified a proline hinge in RNase A with isomerization properties that affects the ability for RNase A to domain-swap [47]. Likewise, McHarg *et al* used site directed mutagenesis to study the role of a proline hinge in yeast phosphoglycerate kinase [25]. In both cases, much like P70A, the mutant variants were less stable than their respective wild type [47, 25], suggesting that the hinge region stabilizes the native fold of the protein [25]. However, unlike KaiB, RNase A and phosphoglycerate kinase have not been identified as metamorphic proteins [2]. Therefore, the destabilized interactions of the native fold proposed by Miller *et al* and McHarg *et al* may only be responsible for a small portion of the effects observed in KaiB. Other works by Subramaniam *et al* and Park *et al* also highlight the active roles of proline hinges in bacteriorhodopsin and buforin II, respectively [72, 8]. Bacteriorhodopsin undergoes a largely localized conformational change that suggest a functional role for proline in the 'switch' mechanism for proton release and uptake [72, 76]. The mechanism for the proline hinge in buforin II is not well understood however, it has been proposed by Xie *et al* that without the proline hinge buforin II cannot undergo translocation thus, decreasing antimicrobial properties [86, 8]. Although still different from the metamorphic characteristics of KaiB, Subramaniam *et al*, Park *et al*, and Xie *et al* all describe functional roles of proline hinges, while Miller *et al* and McHarg *el al* had a stronger focus on the proline hinge contributions to global stability. Based on current knowledge of KaiB, it is likely that Pro^{70} acts both as a stabilizing and functional proline hinge.

When Pro^{70} is mutated to alanine in gsKaiB, it can be inferred that the first turn of the α3 helix becomes more rigid and thus sequentially decrease the flexibility between the coil and the helix. Because of this, it is possible that the stiffening of the α3-coil interaction restricts local sampling of different conformations. This could explain the decreased global stability (as shown by DSC) of P70A KaiB because now that the hinge is removed, thermal fluctuations tend to expose the hydrophobic core (fig. 4.1). Therefore, Pro^{70} helps stabilize KaiB by providing local flexibility in the structure. This flexibility may also be what allows gsKaiB to sample different conformations as it unfolds and refolds to its fold switch state without completely denaturing.

To further test this hypothesis, NMR relaxation can be used to provide information on the molecular motions of KaiB on a per residue bases [(34)]. Prior to running the relaxation experiments on KaiB and the proline-to-alanine mutant variants, a control sample (Ubiquitin) was used to optimize the ^{15}N T_1relaxation experiment. Sample runs on ubiquitin showed that T_1 relaxation measurements were not accurate due to poor water suppression (graph 3.1). The effects of ionic strength on ^{15}N T_1relaxation were also tested. With proper ^{1}H pulse calibration, the sample with higher ionic strength concentration (~45 mM) had lower ^{15}N T_1values than the low ionic strength (~10 mM) sample, rmsd=0.041sec, showing that accurate values may only be obtainable under low salt concentrations, at least for the Bruker TXI cryoprobe.

KaiB is a rare metamorphic protein that uses a fold switching mechanism to adopt two distinct conformations essential to the cyanobacterial circadian clock. The knowledge gained from KaiB's fold switching mechanism could help unravel the mechanistic details

of the entire clock and clock output. For example, studying the fold switching mechanism of KaiB could help explain how the activities of output proteins SasA and CikA are temporally separated. The DSC studies described here suggest a proline trans-cis molecular hinge is required for KaiB stability. Future studies of NMR relaxation of KaiB have the potential to confirm the role of Pro^{70} as a molecular hinge required for stability as well as protein function. For such experiments, the samples should be prepared in a low ionic strength buffer and utilize the "Jinfa-style" ^{1}H pulse calibration method. Following these guidelines will yield accurate and reliable ^{15}N T_1 relaxation values.

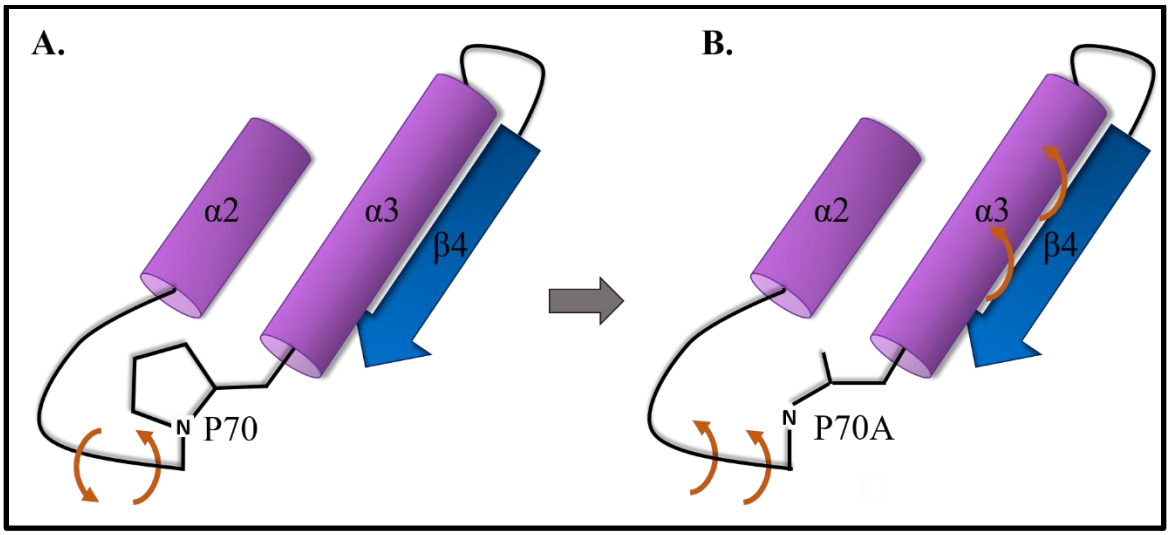

Figure 4.1: (A) Depiction of WT KaiB with a proline residue at 70. The orange arrows represent free movement about the coil without disturbing the α3 helix. (B) KaiB after proline 70 is mutated to alanine. Orange arrows represent movement of the coil and the α3 helix as a unit after stiffening of the proline hinge and exposing the bonds between α3 and β4. It is likely that coil in WT KaiB can move freely leaving the α3 helix near β4, protecting hydrophobic core residues. However, when P70 is mutated to alanine, the coil can no longer move freely subjecting the α3 helix to thermal fluctuation, exposing the core and overall destabilizing KaiB.

METHODS

POLYMERASE CHAIN REACTION

All mutations were made through two step PCR. Fragments were constructed using a “Forward Primer” that was either one of the respective KaiB forward primers (listed in supplementary) or SUMO (I). Similarly, the “Reverse Primer” was either one of the respective KaiB reverse primers or T7 (-). “Fragment 1” and “Fragment 2” represent the products derived from step 1. Fragment products were then combined for overlap extension (step 2). Overlap extension reaction mixtures were made without the addition of SUMO (I) and T7 (-) and ran in the thermocycler for 5 cycles. SUMO (I) and T7 (-) were then added to the reaction and the thermocycler continued for 28 more cycles. Products from overlap extension were digested with restriction enzymes NdeI and HindIII and allowed to incubate at 37℃ for one hour. Restriction enzymes from the digested product mix were removed using a PCR purification kit. Ligation of the digested products used T4 DNA Ligase and pET-28b digested vector (pET-28b-SUMO) cut with NdeI and HindIII from Th. KaiA and incubated at room temperature for three hours. XL1-Blue cells were used for transformation on Millers Luria Broth (LB) plates infused with 50mg/mL Kanamycin. Colonies from transformation were grown in 5 mL of LB for 6 hours followed by plasmid extraction via GeneJet MiniPrep. Plasmids were sent for DNA screening at UC Berkley. After sequence conformation, transformation was done a second time with BL21(DE3) cells. Glycerol stocks of the BL21(DE3) cells were made of each mutation from 400 μL of culture and 100 μL 80% glycerol.

Reaction mixtures and thermocycler program are listed below

Step 1 (Fragments)

16μL Water

Reaction mixture

0.5μL Template TBN99YY 1ng/μL

0.5μL "Forward Primer" 10μM

0.5μL "Reverse Primer" 10μM

2.5μL dNTPs 2mM

5μL 5x Phusion Buffer HF

0.25μL Phusion HF Polymerase

Thermocycler Program

1. 98℃ 30 seconds
2. 98℃ 10 seconds
3. 52℃ 30 seconds
4. 72℃ 2 minutes 30 seconds
5. Step 2-4 repeat, 28 cycles
6. 72℃ 5 minutes
7. 4℃ Hold

Step 2 (Overlap Extension)

16μL water

Reaction Mixture

0.5μL "Fragment 1" 1ng/μL

0.5μL "Fragment 2" 1ng/μL

0.5μL Forward Primer SUMO (I) 10μM

0.5μL Reverse Primer T7 (-) 10μM

2.5μL dNTPs 2mM

5.0μL 5x Phusion Buffer HF

0.25μL Phusion HF Polymerase

Thermocycler Program

1. 98℃ 30 seconds
2. 98℃ 10 seconds
3. 52℃ 30 seconds
4. 72℃ 2 minutes 30 seconds
5. Step 2-4 repeat, 5 cycles then 28 cycles
6. 72℃ 5 minutes
7. 4℃ Hold

Digestion:

20μL of overlap extention product

2.5μL 10x NE Buffer

1μL NdeI

1μL HindIII

Ligation:

5μL digested product

1μL pET-28b-digested vector (pET-28B-SUMO) vector cut NdeI/HindIII from Th. KaiA

1μL 10x T4 DNA ligase buffer

1μL T4 DNA ligase

2μL water

Transformation:

1. 50 μL of XL1-Blue (or BL21(DE3)) competent to 10 μL ligation product (or plasmid)
2. Incubate on ice 30 min
3. Heat shock 45 seconds, 42℃
4. Incubate on ice 2 minutes
5. Add 500 μL pre-warmed 2XYT broth, mix
6. Incubate for one hour, 37℃ 220 rpm
7. Spin cells; 5000 rpm 2 minutes
8. Discard 450 μL supernatant
9. Re-suspend pellet in remaining broth and plate on LB Kan^+ plate
10. Incubate plates: 37℃ overnight

Product Information

5x Phusion Buffer ® HF

Reaction buffer

#B05185S

New England BioLabs

Phusion ® HF DNA Polymerase

#M0530L

New England BioLabs

10x NE Buffer 2

#B7002S New England BioLabs

NdeI

#R011L New England BioLabs

HindIII

#R014L New England BioLabs

10x Buffer T4 DNA ligase buffer

With 10Mm ATP

#B0202S New England BioLabs

T4 DNA ligase

#M0202L

New England BioLabs

GeneJET Gel Extraction Kit #K0692
Thermo Scientific

GeneJET Plasmid Miniprep Kit

#K0503

Thermo Scientific

GeneJET PCR purification Kit

#K0702

Thermo Scientific

PROTEIN EXPRESSION

Miller Luria Broth (LB)

Starting culture made from 2 μL of glycerol stock inoculated into 5 mL of LB with 50mg/mL Kanamycin grown for 6-12 hours at 37°C, 220 rpm. 25g of Millers LB per liter of water (autoclaved) was inoculated with the starting culture. 1 mL of 50 mg/mL of Kanamycin was also added simultaneously. Culture was grown for 3-4 hours at 37°C, 220 rpm. Between 3-4 hours, optical density (OD) was measured at 600nm. Once the OD reached 0.6 the culture was induced with 200 μL of Isopropyl β-D-1-thiogalactopyranoside (IPTG). The culture was then grown for 16 hours at 25°C, 220 rpm. The cells were harvested by spinning at 4°C, 5000 rpm, for ten minutes. The pellets were then re-suspended in equilibration buffer. After harvesting the cells were either prepped for purification or stored at -20°C until ready for purification.

Minimal Media (M9) ^{15}N labelled

The same process is followed as described for LB expression except for growth period and media. The growth period before induction with IPTG was 6-7 hours. The media was made by mixing together in 1L of deionized water 6g Na_2HPO_4, 3g KH_2PO_4, 0.5g NaCl, and 1g NH_4Cl (^{15}N labelled). After autoclaving, 10mL of 20% glucose, 2mL 1M $MgSO_4$, 100 μL 1M $CaCl_2$, and 1mL 50mg/ml Kanamycin were added.

All KaiB samples were expressed using Kanamycin. Ubiquitin was expressed using Ampicillin.

PROTEIN PURIFICATION

Protocol is for 1L of cells harvested from expression. ^{15}N labelled and un-labelled proteins were purified the same except for ubiquitin. Ubiquitin purification was stopped after elution.

Cells harvested from expression were cracked via high pressure homogenizer. The homogenizer used 10,000 – 15,000 bar to crack the cells. The solution was then spun down at 15,000rpm, 4℃, for 30 minutes. The pellet was discarded and the supernatant was poured through a Nickel Column. KaiB was expressed with a Small Ubiquitin-like Modifier (SUMO) fusion protein containing a 6x Histidine tag (His-tag). The His-tag allows for binding to the nickel column. After the supernatant, the nickel column was rinsed with 50 mL of wash buffer. The 20mM imidazole removes any un-specifically bound proteins from the nickel column. SUMO-KaiB was then eluted with 7mL of elution buffer. The elution fraction was incubated for 16 hours with 200μL of 100 μM Ubiquiti-like specific protease 1 (ULP1) to cleave off SUMO from KaiB. The nickel column was then cleaned with water followed by 6M Gnd-HCl, water (3x), and equilibration buffer. The cleaved fraction of SUMO and KaiB in 250 mM imidazole was diluted to 50mL with equilibration buffer and ran through the nickel columns again to separate SUMO from the sample. The flow rate was reduced by clamping a binder clip to the opening of the nickel column modified with plastic tubing. The SUMO bound to the nickel was removed by adding 7mL of elution buffer. The column was then cleaned as before (water, 6M Gnd-HCL, water 3x, equilibration) and the flow through sample from the previous step was passed through the Ni column one more time to eliminate any excess SUMO. After the second nickel column run, KaiB samples were concentrated to ~6mL on a 10KDa membrane and ubiquitin samples were concentrated on a 3KDa membrane also to ~6mL. Size exclusion chromatography was used to separate out the final protein sample. Sample concentrations were measured using a bovine serum albumin (BSA) standard curve.

KaiB DSC samples were purified in 20mM potassium phosphate pH7.4 buffer. Ubiquitin was purified in 20mM Tris-base 50mM NaCl pH7.

Buffers

Equilibration: 50mM Na_2HPO_4, 500mM NaCl, pH 8 buffer

Wash: 50mM Na_2HPO_4, 500mM NaCl, 20mM Imidazole, pH 8 buffer

Elution: 50mM Na_2HPO_4, 500mM NaCl, 250mM Imidazole, pH 8 buffer

6M Gnd-HCl: 6M Guanidine-HCl, 0.2M acetic acid

Product Information

Homogenizer: EmulsiFlex-C3 Avestin® cell disrupter

HPLC: Unicorn 5.10

HiLoad™ 16/600

Superdex™ 75pg

NanoDrop 200 Spectrophotometer

Thermo Scientific

DR6000™ UV VIS Spectrophotometer with RFID Technology

NANO DIFFERENTIAL SCANNING CALORIMETER (DSC)

All samples were tested using the same program, buffer, and concentration

Program

Step	Lower temp (℃)	Higher Temp (℃)	Duration (seconds)	Equilibration (seconds)	Rate ($℃/min$)	Pressure (atm)
1: Heating	25	100	4500	600	1	3.00
2: Cooling	25	100	4500	600	1	3.00
3: Heating	25	100	4500	600	1	3.00
4: Cooling	25	100	4500	600	1	3.00
5: Heating	25	100	4500	600	1	3.00

Buffer

20mM Potassium Phosphate, pH 7.35-7.39, ionic strength 24mM, prepared at 25℃ to be used at 25℃. A phosphate buffer was chosen due to its ability to maintain a stable pH with changes in temperatures. It was also chosen based on the companies (TA Instruments) suggestion as a relatively steady buffer with minimal fluctuations in the baseline.

Sample Preparation

Before testing protein samples, a buffer baseline was tested. For the baseline, 20mM K-Phosphate was loaded into both the 'reference' cell and 'sample' cell. To test the protein samples, two 1 mL aliquots of buffer were degassed for 30 min prior to running the program and used to make a 50μM protein sample. 350µL of the degassed buffer were loaded into the reference cell of the DSC and 350µL of the protein solution were loaded into the sample cell.

Data Analysis

Nano Launch Analyze is the nano DSC specific program designed by TA instruments to process the raw data. The same baseline run was used to analyze all protein samples. A Two State Scaled model was used to fit the data.

Product Information

Nano DSC microcalorimeter
TA Instruments

Launch Nano Analyze
TA Instruments

NUCLEAR MAGNETIC RESONANCE (NMR)

Ubiquitin samples only

Sample Preparation

Both the “high salt” (HS) sample and “low salt” (LS) samples were purified in 20mM Tris-base 50mM NaCl pH7. The HS sample underwent buffer exchange with a 10 mM NaCl solution via concentrator (3KDa membrane) then titrated to pH 7.4 after the NMR sample was prepared using a micro pH meter. For the LS sample, a 1 L of 10mM NaCl solution was titrated to pH 7.4 prior to buffer exchange. After buffer exchange, the ubiquitin sample was prepared for the NMR. Aside from the changes in buffer titration procedure, the samples were both prepared as follows; 5% D_2O, 0.02% NaN_3, 20μM DSS, 1x Protease Inhibitor, and 1.4mM ubiquitin. The samples were then spun at 13,000 rpm for 1 minute to eliminate any air bubbles and injected into a BMS-003 symmetrical microtube (Shigemi tube) and degassed for five minutes. The plunger was then inserted and the final sample volume was set to 19mm in height.

Product Information

Bruker 600 MHz AVANCE III spectrometer equipped with a TCI cryoprobe and z-axis pulsed-field gradient capability

Micro pH meter: Mettler Toledo Micro pH Electrode; S7

Lab 850 Benchtop pH Meter

Protease inhibitor: Complete: cocktail tablets 1 697 498

SUPPLEMENTARY

PCR

Primers

Proline 63 → Alanine (CCT → GCT)

Forward: 5'-gataaaattttggccacggctacccttgccaaagtcc-3'

Reverse: 5'-ggactttggcaagggtagccgtggccaaaattttatc-3'

Proline 70 → Alanine (CCG → GCG)

Forward: 5'-ccttgccaaagtcctagcgcccccctgtgcg-3'

Reverse: 5'-cgcacaggggcgctaggactttggcaagg-3'

Proline 72 → Alanine (CCT → GCT)

Forward: 5'-gtcctaccgcccgctgtgcgccgg-3'

Reverse: 5'-ccggcgcacagcgggcggtaggac-3'

Proline 70 and 72 → Alanine (CCG → GCG; CCT→GCT)

Forward: 5'-caaagtcctagcgcccgctgtgcgccgg-3'

Reverse: 5'-ccggcgcacagcgggcgctaggactttg-3'

P63A-P70A, P63A-P72A, and P63A-P70A-P72A were made by using mutant P63A as the template with primers P70A, P72A or P70A-P72A.

Purification

WT KaiB and proline mutants 17% SDS-PAGE gel.

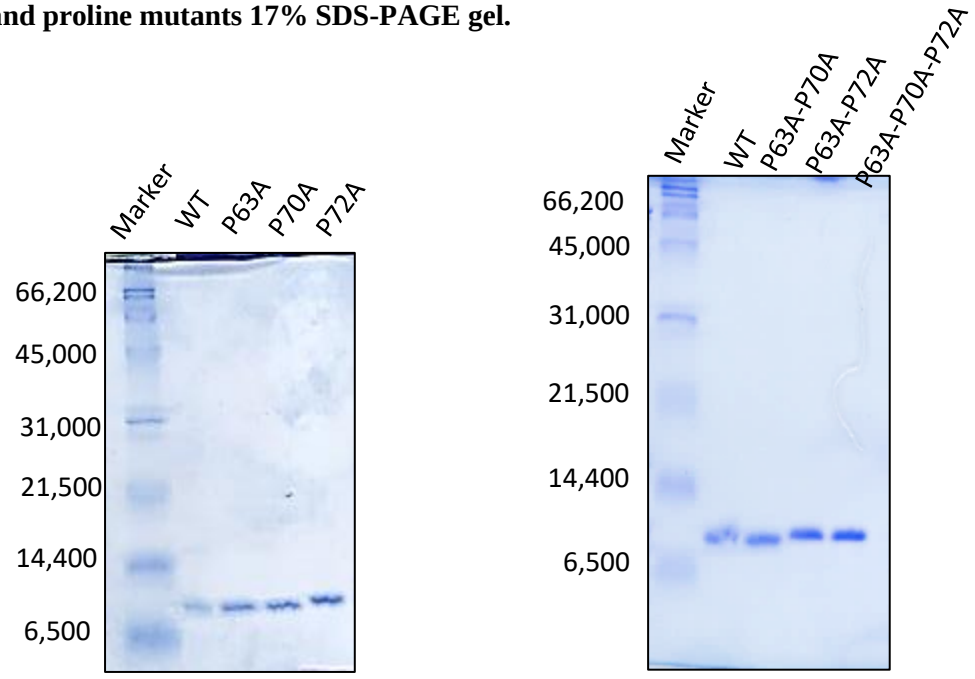

Protein size:

WT KaiB: 10.827KDa (per subunit)

TBN99YY-P63A: 10.84KDa

TBN99YY-P70A: 10.84KDa

TBN99YY-P72A: 10.84KDa

TBN99YY-P63A-P70A: 10.82KDa

TBN99YY-P63A-P72A: 10.82KDa

TBN99YY-P63A-P70A-P72A: 10.79KDa

Size Exclusion Chromatography for WT KaiB and Proline mutants

Elution peak

WT: 74 mL

P63A: 75 mL

P70A: 75 mL

P72A: 75 mL

P63A-P70A: 74 mL

P63A-P72A: 72 mL

P63A-P70A-P72A: 75 mL

WT KaiB

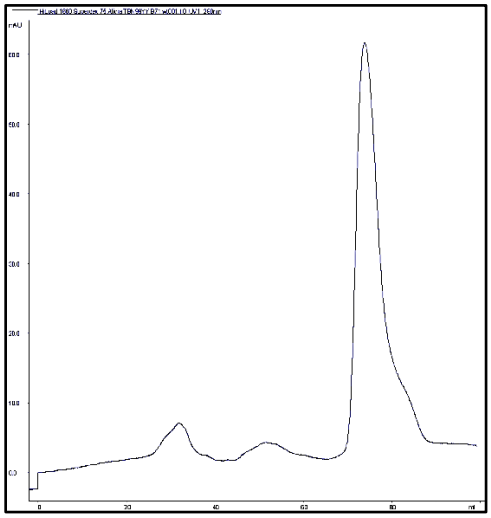

TBN99YY-P70A

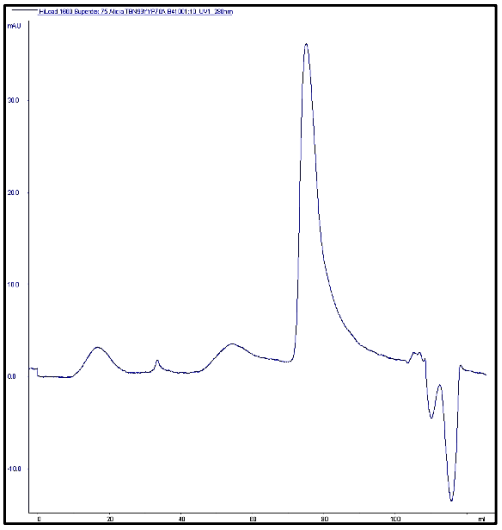

TBN99YY-P63A

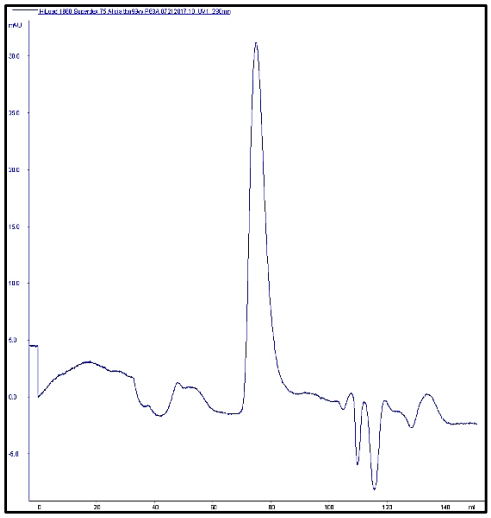

TBN99YY-P72A

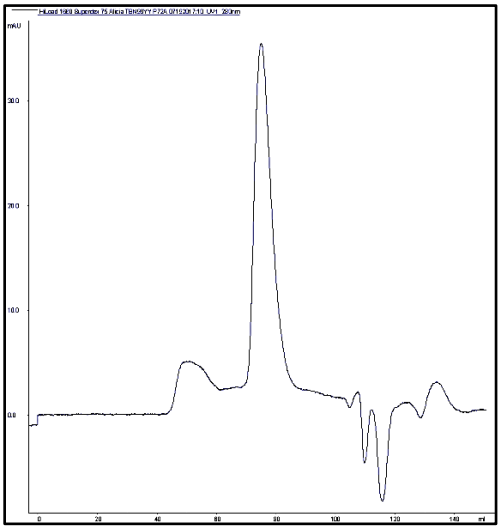

TBN99YY-P63A-P70A

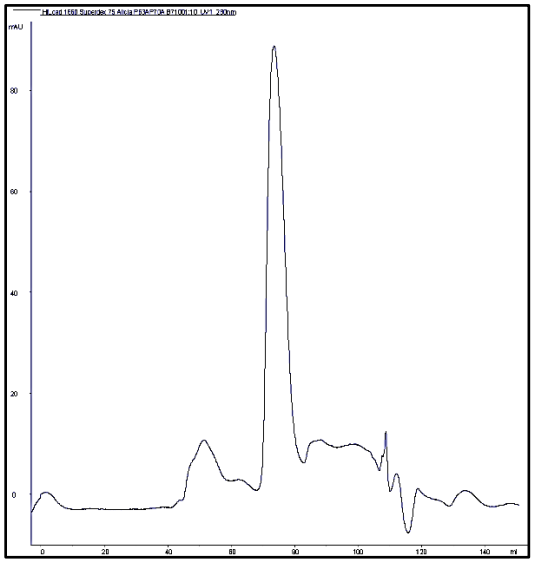

TBN99YY-P63A-P70A-P72A

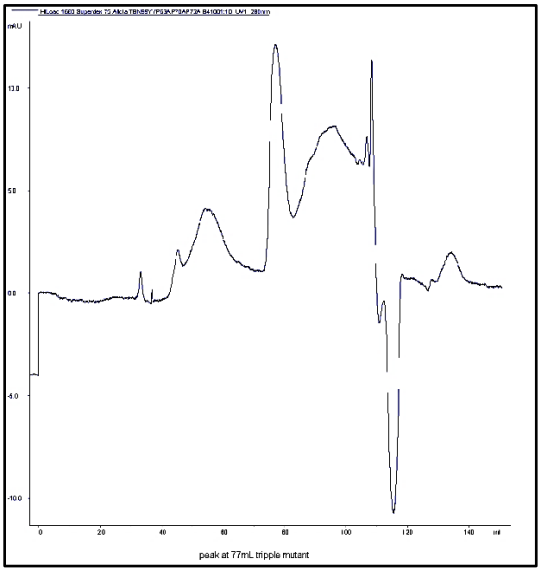

TBN99YY-P63A-P72A

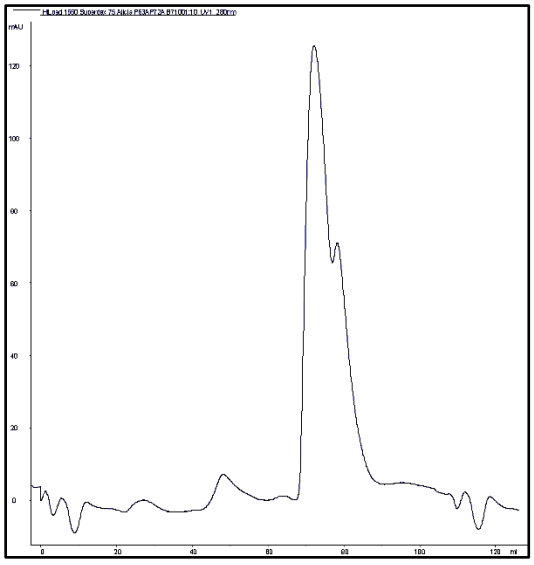

Ubiquitin 17% SDS-PAGE gel and size exclusion chromatography

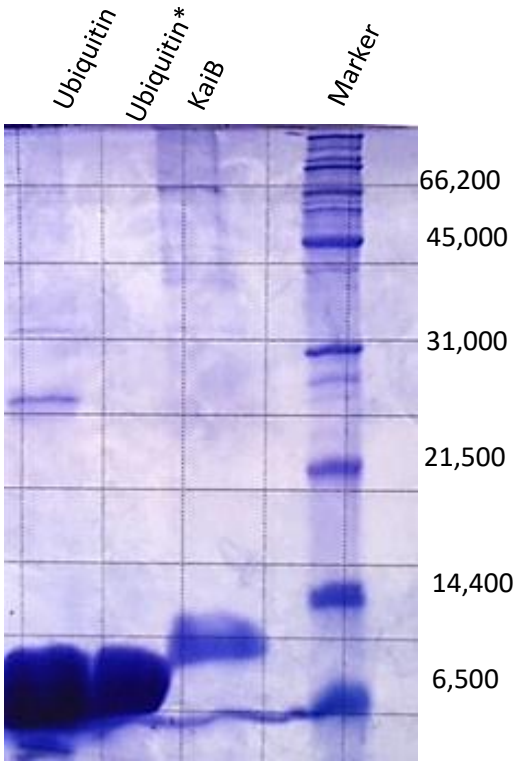

Ubiquitin* = sample after size exclusion chromatography

Ubiquitin = sample pre-size exclusion chromatography

Size of Ubiquitin: 8.5KDa

Elution peak: 90 mL

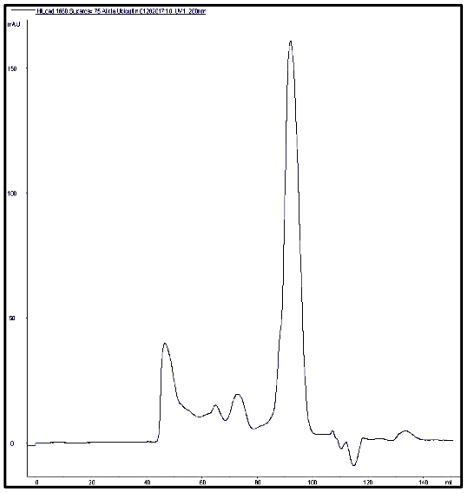

DSC

Overlay of raw data

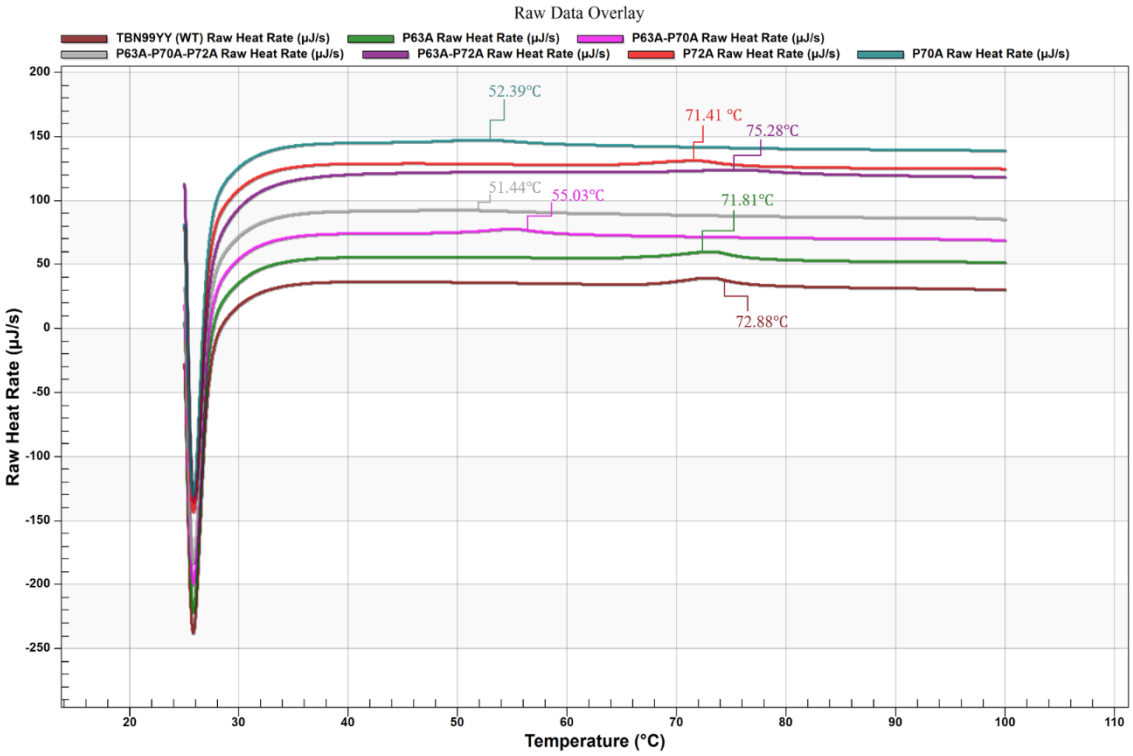

Y-axis is scaled to show all melting profiles staggered.

REFERENCES

1. Abe, J., Hiyama, T. B., Mukaiyama, A., Son, S., Mori, T., Saito, S., Akiyama, S. (2015). Circadian rhythms. atomic-scale origins of slowness in the cyanobacterial circadian clock.*Science (New York, N.Y.), 349*(6245), 312. Retrieved from http://www.ncbi.nlm.nih.gov/pubmed/26113637
2. Alexey G. Murzin. (2008). Metamorphic proteins. *Science*, *320*(5884), 1725-1726. doi:10.1126/science.1158868
3. Anfinsen, C. B. (1973). *Principles that govern the folding of protein chains*
4. Baldwin, R. L. (1996). How hofmeister ion interactions affect protein stability. *Biophysical Journal, 71*(4), 2056-2063. doi:10.1016/S0006-3495(96)79404-3
5. Becktel, W. J., & Schellman, J. A. (1987). Protein stability curves. *Biopolymers, 26*, 1859-1877.
6. Branden, C., & Tooze, J. (1991). *Introduction to protein structure* (3. print. ed.). New York u.a: Garland.
7. Bright, J. N., & Sansom, M. S. P. (2003). The flexing/twirling helix: Exploring the flexibility about molecular hinges formed by proline and glycine motifs in transmembrane helices. *The Journal of Physical Chemistry B, 107*(2), 627-636. doi:10.1021/jp026686u
8. Chan Bae Park, Kwan-Su Yi, Katsumi Matsuzaki, Mi Sun Kim, & Sun Chang Kim. (2000). Structure-activity analysis of buforin II, a histone H2A-derived antimicrobial peptide: The proline hinge is responsible for the cell-penetrating

ability of buforin II. *Proceedings of the National Academy of Sciences of the United States of America, 97*(15), 8245-8250. doi:10.1073/pnas.150518097

9. Chang, Y., Cohen, S. E., Phong, C., Myers, W. K., Kim, Y., Tseng, R., . . . LiWang, A. (2015). Circadian rhythms. A protein fold switch joins the circadian oscillator to clock output in cyanobacteria. *Science (New York, N.Y.), 349*(6245), 324. Retrieved from http://www.ncbi.nlm.nih.gov/pubmed/26113641
10. Cohen, S. E., & Golden, S. S. (2015). Circadian rhythms in cyanobacteria. *Microbiology and Molecular Biology Reviews : MMBR, 79*(4), 373-385. doi:10.1128/MMBR.00036-15
11. Conference Paper, O.*KaiC A-loops affects KaiA and KaiB binding*
12. Damodaran, S., & Kinsella, J. E. (1981). *The effects of neutral salts on the stability of macromolecules: A NEW APPROACH USING A PROTEIN-LIGAND BINDING SYSTEM* The Journal of Biological Chemistry.
13. Dodd, A. N., Salathia, N., Hall, A., Kevei, E., Toth, R., Nagy, F., . . . Webb, A. A. R. (2005). Plant circadian clocks increase photosynthesis, growth, survival, and competitive advantage.*Science, 309*(5734), 630-633. doi:10.1126/science.1115581
14. Dunlap, J. C., Loros, J. J., & DeCoursey, P. J. (2004). *Chronobiology*. Sunderland, Mass: Sinauer.
15. Gillon, W., Garces, R. G., Wu, N., & Pai, E. F. (2004). Anabaena circadian clock proteins KaiA and KaiB reveal a potential common binding site to their partner KaiC. *The EMBO Journal, 23*(8), 1688-1698. doi:10.1038/sj.emboj.7600190

16. Gómez, J., Hilser, V. J., Xie, D., & Freire, E. (1995). The heat capacity of proteins. *Proteins, 22*(4), 404-412. doi:10.1002/prot.340220410
17. Grzesiek, S., & Bax, A. (1993). The importance of not saturating H2O in protein NMR. applications to sensitivity enhancement and NOE measurements *Journal for the American Chemical Society, 115*, 12593-12594.
18. Gutu, A., & O'Shea, E. K. (2013). Two antagonistic clock-regulated histidine kinases time the activation of circadian gene expression. *Molecular Cell, 50*(2), 288. doi:10.1016/j.molcel.2013.02.022
19. Hitomi, K., Oyama, T., Han, S., Arvai, A. S., & Getzoff, E. D. (2005). Tetrameric architecture of the circadian clock protein KaiB. A novel interface for intermolecular interactions and its impact on the circadian rhythm. *The Journal of Biological Chemistry, 280*(19), 19127-19135. doi:10.1074/jbc.M411284200
20. Höhne, G., Flammersheim, H., & Hemminger, W. (2003). *Differential scanning calorimetry* Berlin: Springer.
21. Ibarra-Molero, B., Loladze, V. V., Makhatadze, G. I., & Sanchez-Ruiz, J. M. (1999). Thermal versus guanidine-induced unfolding of ubiquitin. an analysis in terms of the contributions from charge-charge interactions to protein stability. *Biochemistry, 38*(25), 8138-8149. doi:10.1021/bi9905819
22. Ioannis Vakonakis, Andy C. LiWang, & J. Woodland Hastings. (2004). Structure of the C-terminal domain of the clock protein KaiA in complex with a KaiC-derived peptide: Implications for KaiC regulation. *Proceedings of the National*

Academy of Sciences of the United States of America, *101*(30), 10925-10930. doi:10.1073/pnas.0403037101

23. Iwasaki, H., Williams, S. B., Kitayama, Y., Ishiura, M., Golden, S. S., & Kondo, T. (2000). A KaiC-interacting sensory histadine kinase. SasA, necessary to sustain robust circadian oscillation in cyanobacteria. *Cell*, *101*, 223-233. doi:10.1093/analys/anw017
24. J B Stock, A J Ninfa, & A M Stock. (1989). Protein phosphorylation and regulation of adaptive responses in bacteria. *Microbiological Reviews, 53*(4), 450-490. Retrieved from http://mmbr.asm.org/content/53/4/450.abstract
25. J McHarg, S M Kelly, N C Price, A Cooper, & J A Littlechild. (1999). Site-directed mutagenesis of proline 204 in the 'hinge' region of yeast phosphoglycerate kinase. *European Journal of Biochemistry, 259*(3), 939-945. Retrieved from http://www.ncbi.nlm.nih.gov/pubmed/10092885
26. Jackson, S. E. (1998). How do small single-domain proteins fold? *Folding and Design, 3*(4), R91. doi:10.1016/S1359-0278(98)00033-9
27. Jarymowycz, V. A., & Stone, M. J. (2006). Fast time scale dynamics of protein backbones: NMR relaxation methods, applications, and functional consequences. *Chemical Reviews, 106*(5), 1624-1671. doi:10.1021/cr040421p
28. Jenny Lin, Justin Chew, Udaysankar Chockanathan, & Michael J. Rust. (2014). Mixtures of opposing phosphorylations within hexamers precisely time feedback in the cyanobacterial circadian clock. *Proceedings of the National Academy of Sciences, 111*(37), E3945. doi:10.1073/pnas.1408692111

29. JohnA.Schellman. (1987). The thermodynamic stabilitoyf proteins. *Annual Review of Biophysics, 16,* 115-137.

30. Joost Snijder, Rebecca J. Burnley, Anika Wiegard, Adrien S. J. Melquiond, Alexandre M. J. J. Bonvin, Ilka M. Axmann, & Albert J. R. Heck. (2014). Insight into cyanobacterial circadian timing from structural details of the KaiB—KaiC interaction. *Proceedings of the National Academy of Sciences of the United States of America, 111*(4), 1379-1384. doi:10.1073/pnas.1314326111

31. Kay, L. E., Nicholson, L. K., Delaglio, F., Bax, A., & Torchia, D. A. (1992). Pulse sequences for removal of the effects of cross correlation between dipolar and chemical-shift anisotropy relaxation mechanisms on the measurement of heteronuclear T 1 and T 2 values in proteins. *Journal of Magnetic Resonance (1969), 97*(2), 359-375. doi:10.1016/0022-2364(92)90320-7

32. Kay, L. E., Torchia, D. A., & Bax, A. (1989). *Backbone dynamics of proteins as studied by 15N inverse detected heteronuclear NMR spectroscopy: Application to staphylococcal nuclease"1"* American Chemistry Society.

33. Kay, L. E., Xu, G. Y., & Yamazaki, T. (1994). *Enhanced-sensitivity triple-resonance spectroscopy with minimal H2O saturation * Journal of Magnetic Resonance.

34. Keeler, J. (2012). *Understanding NMR spectroscopy* (2. ed., reprinted ed.). Chichester: Wiley.

35. Kelly, A. E., Ou, H. D., Withers, R., & Dötsch, V. (2002). Low-conductivity buffers for high-sensitivity NMR measurements. *Journal of the American Chemical Society, 124*(40), 12013-12019. doi:10.1021/ja026121b

36. Kondo, T., & Ishiura, M. (2000). The circadian clock of cyanobacteria. *BioEssays : News and Reviews in Molecular, Cellular and Developmental Biology, 22*(1), 10-15. doi:AID-BIES4>3.0.CO;2-A

37. Kondo, T., Tsinoremas, N. F., Golden, S. S., Johnson, C. H., Kutsuna, S., & Ishiura, M. (1994). Circadian clock mutants of cyanobacteria *Science, 266*

38. Kufareva, I., & Abagyan, R. (2012). Methods of protein structure comparison. *Methods in Molecular Biology (Clifton, N.J.), 857*, 231. Retrieved from http://www.ncbi.nlm.nih.gov/pubmed/22323224

39. Kuo, N. (2011). *KaiC CII ring flexibility governs the rhythm of the circadian clock of cyanobacteria* Available from ProQuest Dissertations and Theses Professional. Retrieved from http://search.proquest.com/docview/885662851

40. Lakomek, N., Ying, J., & Bax, A. (2012). Measurement of 15N relaxation rates in perdeuterated proteins by TROSY-based methods. *Journal of Biomolecular NMR, 53*(3), 209-221. doi:10.1007/s10858-012-9626-5

41. Levitt, M. H. (2008). *Spin dynamics* (2. Aufl. ed.). GB: Wiley. Retrieved from http://ebooks.ciando.com/book/index.cfm/bok_id/495883

42. Lewis E Kay. (1998). Protein dynamics from NMR. *Biochemistry and Cell Biology, 76*(2/3), 145-152. doi:10.1139/bcb-76-2-3-145

43. Li, Y., & Montelione, G. T. (1994). Overcoming solvent saturation-transfer artifacts in protein NMR at neutral pH. application of pulsed field gradients in measurements of 1H-15-N overhauser effects *Journal of Magnetic Resonance, Series B 105.1*, 45-51.

44. Martin, J. L. (1995). *Thioredoxin —a fold for all reasons*. ENGLAND: Elsevier Inc. doi:10.1016/S0969-2126(01)00154-X

45. Masahiro Ishiura, Shinsuke Kutsuna, Setsuyuki Aoki, Hideo Iwasaki, Carol R. Andersson, Akio Tanabe, . . . Takao Kondo. (1998). Expression of a gene cluster kaiABC as a circadian feedback process in cyanobacteria. *Science, 281*(5382), 1519-1523. doi:10.1126/science.281.5382.1519

46. Matthews, B. W., Nicholson, H., & Becktel, W. J. (1987). Enhanced protein thermostability from site-directed mutations that decrease the entropy of unfolding. *Proc. Natl. Acad. Sci. Biochemistry, 84*, 6663-6667.

47. Miller, K. H., Karr, J. R., & Marqusee, S. (2010). A hinge region cis-proline in ribonuclease A acts as a conformational gatekeeper for C-terminal domain swapping. *Journal of Molecular Biology, 400*(3), 567-578. doi:10.1016/j.jmb.2010.05.017

48. Morf, J., & Schibler, U. (2010). Circadian cell-cycle progression: Cracking open the gate. *Cell, 140*(4), 458-459. doi:10.1016/j.cell.2010.02.002

49. Muskett, F. W. (2011). *Protein NMR spectroscopy: Principles techniques and applications* Wiley.

50. Nakajima, M., Imai, K., Ito, H., Nishiwaki, T., Murayama, Y., Iwasaki, H., . . . Kondo, T. (2005). Reconstitution of circadian oscillation of cyanobacterial KaiC phosphorylation in vitro.*Science, 308*(5720), 414-415. doi:10.1126/science.1108451

51. Naoki Takai, Masato Nakajima, Tokitaka Oyama, Ryotaku Kito, Chieko Sugita, Mamoru Sugita, . . . Hideo Iwasaki. (2006). A KaiC-associating SasA-RpaA two-

component regulatory system as a major circadian timing mediator in cyanobacteria. *Proceedings of the National Academy of Sciences of the United States of America, 103*(32), 12109-12114. doi:10.1073/pnas.0602955103

52. Nick Pace, C., & Martin Scholtz, J. (1998). A helix propensity scale based on experimental studies of peptides and proteins. *Biophysical Journal, 75*(1), 422-427. doi:10.1016/S0006-3495(98)77529-0
53. Nishiwaki, T., & Kondo, T. (2012). Circadian autodephosphorylation of cyanobacterial clock protein KaiC occurs via formation of ATP as intermediate. *The Journal of Biological Chemistry, 287*(22), 18030. Retrieved from http://www.ncbi.nlm.nih.gov/pubmed/22493509
54. Ono, T., & Hirose, K. (2005). First-principles study of dielectric properties of bulk NaCl and ultrathin NaCl films under a finite external electric field. *Physical Review B, 72*(8) doi:10.1103/PhysRevB.72.085105
55. Pattanayek, R., & Egli, M. (2015). Protein-protein interactions in the cyanobacterial circadian clock: Structure of KaiA dimer in complex with C-terminal KaiC peptides at 2.8 Å resolution.*Biochemistry*, *54*(30), 4575. Retrieved from http://www.ncbi.nlm.nih.gov/pubmed/26200123
56. Pattanayek, R., Wang, J., Mori, T., Xu, Y., Johnson, C. H., & Egli, M. (2004). Visualizing a circadian clock protein:Crystal structure of KaiC and functional insights. *Molecular Cell, 15*(3), 375-388. doi:10.1016/j.molcel.2004.07.013
57. Privalov, P. L., & Potekhin, S. A. (1987). *Scanning microcalorimetry in studying temperature-induced changes in proteins*. Totowa: Humana Press. doi:10.1385/0896031055

58. Rachelle M. Smith, & Stanly B. Williams. (2006). Circadian rhythms in gene transcription imparted by chromosome compaction in the cyanobacterium synechococcus elongatus.*Proceedings of the National Academy of Sciences of the United States of America, 103*(22), 8564-8569. doi:10.1073/pnas.0508696103
59. Robbyn L. Tuinstra, Francis C. Peterson, Snjezana Kutlesa, E. Sonay Elgin, Michael A. Kron, & Brian F. Volkman. (2008). Interconversion between two unrelated protein folds in the lymphotactin native state. *Proceedings of the National Academy of Sciences of the United States of America, 105*(13), 5057-5062. doi:10.1073/pnas.0709518105
60. Robert L. Baldwin. (1986). Temperature dependence of the hydrophobic interaction in protein folding. *Proceedings of the National Academy of Sciences of the United States of America, 83*(21), 8069-8072. doi:10.1073/pnas.83.21.8069
61. Roberts, G. C. K. (1993). *NMR of macromolecules*. Oxford [u.a.]: Univ. Press.
62. Rollins, G. C., & Dill, K. A. (2014). General mechanism of two-state protein folding kinetics. *Journal of the American Chemical Society, 136*(32), 11420. Retrieved from http://www.ncbi.nlm.nih.gov/pubmed/25056406
63. Rule, G. S., & Hitchens, T. K. (2006). *Fundamentals of protein NMR spectroscopy*. Dordrecht: Springer.
64. Ryo Iwase, Katsumi Imada, Fumio Hayashi, Tatsuya Uzumaki, Megumi Morishita, Kiyoshi Onai, . . . Masahiro Ishiura. (2005). Functionally important substructures of circadian clock protein KaiB in a unique tetramer complex. *Journal of Biological Chemistry, 280*(52), 43141-43149. doi:10.1074/jbc.M503360200

65. S.P. Sansom, M., & Weinstein, H. (2000). *Hinges, swivels and switches: The role of prolines in signalling via transmembrane α-helices*. England: Elsevier Ltd. doi:10.1016/S0165-6147(00)01553-4

66. Santoro, M. M., Liu, Y., Khan, S. M. A., Hou, L., & Bolen, D. W. (1992). Increased thermal stability of proteins in the presence of naturally occurring osmolytes *American Chemical Society, 31*(23), 5278-5283.

67. Schmitz, O., Katayama, M., Williams, S. B., Kondo, T., & Golden, S. S. (2000). CikA, a bacteriophytochrome that resets the cyanobacterial circadian clock. *Science, 289*(5480), 765-768. doi:10.1126/science.289.5480.765

68. Senadhi Vijay-Kumar3, 4., Charles E. Bugg, 3, 4, & William J. Cook'7 3v4.*Structure of ubiquitin refined at 143A resolution*

69. Sheng Ye, Ioannis Vakonakis, Thomas R. Ioerger, Andy C. LiWang, & James C. Sacchettini. (2004). Crystal structure of circadian clock protein KaiA from synechococcus elongatus.*Journal of Biological Chemistry, 279*(19), 20511. doi:10.1074/jbc.M400077200

70. Silberberg, M. S. (2006). *Chemistry* (5. ed. ed.). Dubuque, IA: McGraw-Hill.

71. Skelton, N. J., Cavanagh, J., Palmer, I., Arthur G, & Fairbrother, W. J. (1995). *Protein NMR spectroscopy* (2nd ed.). Saint Louis: Academic Press. Retrieved from http://lib.myilibrary.com?ID=276887

72. Subramaniam, S., & Henderson, R. (2000). Molecular mechanism of vectorial proton translocation by bacteriorhodopsin. *Nature, 406*(6796), 653-657. doi:10.1038/35020614

73. Taeko Nishiwaki, Hideo Iwasaki, Masahiro Ishiura, & Takao Kondo. (2000). Nucleotide binding and autophosphorylation of the clock protein KaiC as a circadian timing process of cyanobacteria. *Proceedings of the National Academy of Sciences of the United States of America*, *97*(1), 495-499. doi:10.1073/pnas.97.1.495

74. Tetsuya Mori, Brian Binder, & Carl Hirschie Johnson. (1996). Circadian gating of cell division in cyanobacteria growing with average doubling times of less than 24 hours. *Proceedings of the National Academy of Sciences of the United States of America*, *93*(19), 10183-10188. doi:10.1073/pnas.93.19.10183

75. Thammajun L. Wood, Jennifer Bridwell-Rabb, Yong-Ick Kim, Tiyu Gao, Yong-Gang Chang, Andy LiWang, . . . Steven L. McKnight. (2010). The KaiA protein of the cyanobacterial circadian oscillator is modulated by a redox-active cofactor. *Proceedings of the National Academy of Sciences of the United States of America*, *107*(13), 5804-5809. doi:10.1073/pnas.0910141107

76. Tieleman, D. P., Shrivastava, I. H., Ulmschneider, M. R., & Sansom, M. S. P. (2001). Proline-induced hinges in transmembrane helices: Possible roles in ion channel gating. *Proteins: Structure, Function, and Bioinformatics*, *44*(2), 63-72. doi:10.1002/prot.1073

77. Tjandra, N., Feller, S. E., Pastor, R. W., & Bax, A. (1995). Rotational diffusion anisotropy of human ubiquitin from N NMR relaxation. *Journal of the American Chemical Society*, *117*(50), 12562.

78. Tseng, R., Chang, Y., Bravo, I., Latham, R., Chaudhary, A., Kuo, N., & Liwang, A. (2014). Cooperative KaiA-KaiB-KaiC interactions affect KaiB/SasA

competition in the circadian clock of cyanobacteria *Journal of Molecular Biology, 426*, 389-402.

79. Tseng, R., Goularte, N. F., Chavan, A., Luu, J., Cohen, S. E., Chang, Y., . . . Partch, C. L. (2017). Structural basis of the day-night transition in a bacterial circadian clock. *Science, 355*(6330), 1174. doi:10.1126//science.aag2516
80. Tzeng, S., Sarkar, P., Kalodimos, C. G., Birge, R. B., & Saleh, T. (2011). Structural basis for regulation of the crk signaling protein by a proline switch. *Nature Chemical Biology, 7*(1), 51-57. doi:10.1038/nchembio.494
81. Valencia S, J., Bitou, K., Ishii, K., Murakami, R., Morishita, M., Onai, K., . . . Ishiura, M. (2012). Phase-dependent generation and transmission of time information by the KaiABC circadian clock oscillator through SasA-KaiC interaction in cyanobacteria. *Genes to Cells, 17*(5), 398-419. doi:10.1111/j.1365-2443.2012.01597.x
82. Villarreal, S. A., Pattanayek, R., Williams, D. R., Mori, T., Qin, X., Johnson, C. H., . . . Stewart, P. L. (2013). CryoEM and molecular dynamics of the circadian KaiB-KaiC complex indicates that KaiB monomers interact with KaiC and block ATP binding clefts. *Journal of Molecular Biology, 425*(18), 3311-3324. doi:10.1016/j.jmb.2013.06.018
83. Wang, J. (2004). Nucleotide-dependent domain motions within rings of the RecA/AAA+ superfamily. *Journal of Structural Biology, 148*(3), 259-267. doi:10.1016/j.jsb.2004.07.003
84. Willians, S. B., Vakonakis, I., Golden, S. S., & LiWang, A. C. (2002). Structure and function form the circadian clock protein KaiA of *synechococcus*

elongatus: A potential clock input mechanism *Pnas, 99*(24), 15357-15362.

85. Wu, P. S. C., & Otting, G. (2005). Rapid pulse length determination in high-resolution NMR. *Journal of Magnetic Resonance, 176*(1), 115-119. doi:10.1016/j.jmr.2005.05.018
86. Xie, Y., Fleming, E., Chen, J. L., & Elmore, D. E. (2011). Effect of proline position on the antimicrobial mechanism of buforin II. *Peptides, 32*(4), 677-682. doi:10.1016/j.peptides.2011.01.010
87. Yong-Gang Chang, Roger Tseng, Nai-Wei Kuo, & Andy LiWang. (2012). Rhythmic ring-ring stacking drives the circadian oscillator clockwise. *Proceedings of the National Academy of Sciences of the United States of America, 109*(42), 16847-16851. doi:10.1073/pnas.1211508109
88. Yong-Ick Kim, Guogang Dong, Carl W. Carruthers, Susan S. Golden, & Andy LiWang. (2008). The day/night switch in KaiC, a central oscillator component of the circadian clock of cyanobacteria. *Proceedings of the National Academy of Sciences of the United States of America, 105*(35), 12825-12830. doi:10.1073/pnas.0800526105
89. Rust, M. J., Markson, J. S., Lane, W. S., Fisher, D. S., & O'Shea, E. K. (2007). Ordered phosphorylation governs oscillation of a three-protein circadian clock. *Science, 318*(5851), 809-812. doi:10.1126/science.1148596
90. Kazuki Terauchi, Yohko Kitayama, Taeko Nishiwaki, Kumiko Miwa, Yoriko Murayama, Tokitaka Oyama, & Takao Kondo. (2007). ATPase activity of KaiC determines the basic timing for circadian clock of cyanobacteria. *Proceedings of the National Academy of Sciences of the United States of America, 104*(41), 16377-16381. doi:10.1073/pnas.0706292104